T.R.
USKUDAR UNIVERSITY
INSTITUTE OF SCIENCE

DEPARTMENT OF MOLECULAR BIOLOGY
MASTER'S DEGREE OF MOLECULAR BIOLOGY
MASTER'S DEGREE THESIS

INVESTIGATION OF THE ANTI-INFLAMMATORY EFFECT OF UMBILICAL CORD MESENCHYMAL STEM CELL-DERIVED EXOSOMES ENRICHED WITH QUERCETIN ON A NEUROINFLAMMATION MODEL USING LPS-INDUCED MICROGLIA HMC3 CELL LINE

Sajeda OSMAN

Thesis Advisor
Prof. Dr. Sevim IŞIK

Thesis Co-Advisor
Doç. Dr. Gülen Melike DEMİRBOLAT

İSTANBUL-2025

T.R.
USKUDAR UNIVERSITY
INSTITUTE OF SCIENCE

DEPARTMENT OF MOLECULAR BIOLOGY
MASTER'S DEGREE OF MOLECULAR BIOLOGY
MASTER'S DEGREE THESIS

INVESTIGATION OF THE ANTI-INFLAMMATORY EFFECT OF UMBILICAL CORD MESENCHYMAL STEM CELL-DERIVED EXOSOMES ENRICHED WITH QUERCETIN ON A NEUROINFLAMMATION MODEL USING LPS-INDUCED MICROGLIA HMC3 CELL LINE

Sajeda OSMAN

Thesis Advisor
Prof. Dr. Sevim IŞIK

Thesis Co-Advisor
Doç. Dr. Gülen Melike DEMİRBOLAT

This research was supported by TÜSEB A2 group project with project number 43313.

İSTANBUL-2025

ÖZET

KUERSETİN İLE ZENGİNLEŞTİRİLMİŞ KORDON KAYNAKLI MEZENKİMAL KÖK HÜCRE EKSOZOMLARININ, LPS İNDÜKLÜ HMC3 MİKROGLİA NÖROİNFLAMASYON MODELİNDE, ANTİENFLAMATUAR ETKİSİNİN İNCELENMESİ

Nöroinflamasyon, henüz tedavisi bulunamamış olan nörodejeneratif hastalıkların gelişiminde rol oynayan kritik bir patofizyolojik süreçtir. Bağışıklık hücreleri, özellikle mikroglia, merkezi sinir sistemindeki inflamatuar yanıtların ana düzenleyicileridir. Nörodejeneratif hastalıklarda mikroglia'nın rolünün daha iyi anlaşılması, etkili tedavilerin geliştirilmesi için esastır, çünkü karmaşık hastalıklar karmaşık tedaviler gerektirir. Önceki çalışmalar, GK-MKH kökenli eksozomların nöroinflamasyonu azaltmada terapotik etkisini göstermiştir. Benzer şekilde, kuersetin antioksidan, anti-inflamatuar ve nörokoruyucu etkiler gösterir ve nöroinflamasyonu azaltmada önemli bir rol oynar.

Bu çalışmada, kuersetin yüklü eksozomların (Que-Exo) LPS ile indüklenen nöroinflamasyon modelindeki anti-inflamatuar etkilerinin araştırılması amaçlanmıştır. Bu hipotez; hücre canlılığının değerlendirilmesi için MTT analizi, pro-inflamatuar sitokin analizi için, nitrit düzeyleri için Griess analizi, iNOS enzim aktivitesi, sitoplazmik NF-κB, iNOS ve COX-2 protein ekspresyonları için Western blot dahil olmak üzere çeşitli moleküler analizlerle desteklenmiştir.

Sonuçlar, Que-Exo ön uygulamasının hücre canlılığını önemli ölçüde iyileştirdiğini ve LPS ile indüklenen inflamatuar yanıtları azalttığını göstermiştir. Özellikle, Que-Exo uygulaması NF-κB sinyal yolunun aktivasyonunu artırırken, nitrit, iNOS ve COX-2 düzeylerini düşürmüş ve pro-inflamatuar sitokin ekspresyonlarını baskılamıştır.

Bu bulgular, Que-Exo'nun kuersetinin biyoaktif özellikleri ile GK-MKH kökenli eksozomların hedefe yönelik taşıma kapasitesini birleştirerek sinerjik bir

antienflamatuar etki gösterdiğini ve nöroinflamasyonu hafifletmede etkili bir tedavi ajanı olabileceğini göstermektedir.

Anahtar Kelimeler: Nöroinflamasyon, Lipopolisakkarit, Mikroglia, HMC3, Eksozom, Mezenkimal kök hücre, Göbek Kordon, Antioksidan, Kuersetin

ABSTRACT

INVESTIGATION OF THE ANTI-INFLAMMATORY EFFECT OF UMBILICAL CORD MESENCHYMAL STEM CELL-DERIVED EXOSOMES ENRICHED WITH QUERCETIN ON A NEUROINFLAMMATION MODEL USING LPS-INDUCED MICROGLIA HMC3 CELL LINE

Neuroinflammation is a critical pathophysiological process implicated in the development of neurodegenerative diseases, for which cures have not been discovered yet. Among the immune cells involved, microglia serve as primary regulators of inflammation within the central nervous system. Gaining deeper insight into microglial function in these conditions is crucial for the development of targeted and effective therapeutic strategies, especially given the complexity of such diseases. Previous studies have demonstrated the therapeutic effect of exosomes derived from umbilical cord-mesenchymal stem cells in diminishing neuroinflammation. Likewise, quercetin exhibits neuroprotective, antioxidant, and anti-inflammatory properties that contribute to its ability to mitigate neuroinflammatory responses.

This study aimed to evaluate the anti-inflammatory effects of quercetin-loaded exosomes in a neuroinflammation model induced by LPS. This hypothesis was supported by conducting molecular analysis, including MTT assay for cell viability, pro-inflammatory cytokine analysis, Griess assay for nitrite levels, COX-2 and iNOS enzyme activity assays, and Western blotting for cytoplasmic NF-κB, COX-2, and iNOS protein expressions.

The results demonstrated that pretreatment with quercetin-loaded exosomes significantly improved cell viability and reduced LPS-induced inflammatory responses. Notably, quercetin-loaded exosomes increaesd the expression of cytoplasmic NF-κB, reduced nitrite levels, iNOS enzyme activity, iNOS and COX-2 protein expressions, and downregulated the expression of pro-inflammatory cytokine IL-6.

These findings suggest that quercetin-loaded exosomes provide a synergistic anti-inflammatory effect by combining the bioactive properties of quercetin with the

targeted delivery capability of mesenchymal stem cell-derived exosome, which serve as an effective therapeutic agent for mitigating neuroinflammation.

Keywords: Neuroinflammation, Lipopolysaccharide, Microglia, Exosome, Mesenchymal stem cell, Umbilical Cord, Antioxidant, Quercetin

ACKNOWLEDGEMENT

I would like to extend my deepest gratitude to my MSc supervisor, Prof. Dr. Sevim IŞIK, whose support and guidance made this work possible. I am profoundly grateful for the opportunity she provided me to conduct research under her supervision. My heartfelt thanks also go to my co-advisor, Dr. Gülen Melike DEMİRBOLAT, for her genuine support and invaluable contributions to the successful completion of this thesis.

I am sincerely grateful to Dr. Berçem YEMAN KIYAK, manager of ÜSKÖKMER, as well as to my laboratory mates, Aya SAHSAHI, Suhair SHAMSHIR, Nesrin EDWAN SÁNCHEZ, and Sedra ALHELWANI, whose encouragement and willingness to share knowledge significantly enriched my learning experience.

A special thanks to my beloved family, whose unwavering support has been the backbone of my academic journey. I am deeply indebted to my father, Ghaleb OSMAN, and my mother, Fadia AYOUBI, for their unconditional love and encouragement. I am also grateful to my sister, Sarah, and my brothers, Osman, Moaz, and Mohammad OSMAN, for their continuous support.

I sincerely thank TÜSEB for their generous support of my master's research project (No. 43313), entitled "Investigation of the Anti-inflammatory Effect of Umbilical Cord Mesenchymal Stem Cell-Derived Exosomes Enriched with Quercetin on a Neuroinflammation Model Using LPS-Induced Microglia HMC3 Cell Line." Their funding enabled me to carry out this research successfully.

Lastly, I would like to thank everyone who supported me in any way during this research journey, whether directly or indirectly. Their contributions, no matter how small they were, have been deeply appreciated and valued.

DECLARATION

I hereby declare that the thesis entitled “Investigation of the Anti-Inflammatory Effect of Umbilical Cord Mesenchymal Stem Cell-Derived Exosomes Enriched with Quercetin on a Neuroinflammation Model Using LPS-Induced Microglia HMC3 Cell Line” is the result of my independent research. This work has not been previously submitted, in whole or in part, for the award of any academic degree or professional qualification at any other institution.

I further affirm that all sources of information, data, and scholarly content have been duly cited and acknowledged in accordance with the principles of academic honesty and ethical research conduct. This thesis fully complies with the institutional standards of academic integrity and responsible authorship.

07/07/2025

Sajeda OSMAN

CONTENTS

INDEX OF TABLES

Page

INDEX OF FIGURES

Page

INDEX OF ABBREVIATIONS

AD: Alzheimer's disease

AKT: Protein kinase B

ALIX: ALG-2 interacting protein X

AMPK: AMP-activated protein kinase

ANXA2: Calcium-regulated membrane-binding protein

Arg-1: Arginase-1

ATP: Adenosine triphosphate

Bax: Bcl-2-associated X protein

BBB: Blood-brain barrier

Bcl-2: B-cell lymphoma 2

BV2: Murine-derived microglia clone-3 cell line

CD: Tetraspanin cluster of differentiation

CD206: Mannose receptor

CNS: Central nervous system

COX-1: Cyclooxygenase-1

COX-2: Cyclooxygenase-2

DAPI: 4′,6-diamidino-2-phenylindole

DMSO: Dimethyl Sulfoxide

eEMP: Early erythroid myeloid progenitor

ERK1/2: Extracellular signal-regulated kinase 1 and 2

EV: Extracellular vesicle

Exo: Exosome

Fas: Fas ligand

FBS: Fetal bovine serum

FIZZ1: Found in inflammatory zone 1

HD: Huntington's disease

HMC3: Human microglia cell line

HO-1: Heme oxygenase-1

HSP: Heat shock protein

IFN-γ: Interferon-gamma

IGF-1: Insulin-like growth factor 1

IL: Interleukin

ILV: Intraluminal vesicle

iNOS: inducible nitric oxide synthase

IκBα: NF-κB inhibitor alpha

LPS: Lipopolysaccharide

MAPK: Mitogen-activated protein kinase

MEM: Modified eagle's medium

MHC-I: Histocompatibility complex class I

MHC-II: Histocompatibility complex class II

MSC: Mesenchymal stem cell

mTOR: Mammalian target of rapamycin

MVB: Multivesicular body

NFκB: Nuclear factor kappa B

NI: Neuroinflammation

NLRP3: NOD-like receptor pyrin domain-containing protein 3

Nrf2: Nuclear factor E2-related factor 2

p53: Tumor protein P53

PBS: Phosphate buffered saline

PD: Parkinson's disease

PI3K: Phosphoinositide 3-kinase

PLC: Phospholipase C

Que: Quercetin

Que-Exo: Quercetin-loaded exosome

Rab: Ras-associated binding

RhoA: Ras homolog gene family member A

ROS: Reactive oxygen species

SIRT1: NAD-dependent deacetylase sirtuin-1

SNARE: Soluble NSF-attachment protein receptor

TGF-β: Transforming growth factor-β

TLR: Toll-like receptor

TNF-α: Tumor necrosis factor-alpha

TRAIL: TNF-related apoptosis-inducing ligand

TREM2: Triggering receptor expressed on myeloid cells 2

TSG101: Tumor susceptibility gene 101

UC: Umbilical cord

VPS4: Vacuolar protein sorting-associated protein

WJ: Wharton jelly

Ym-1: Chitinase 3-like

1. INTRODUCTION

Neuroinflammation is a complex and sustained immune response that occurs in the central nervous system (CNS), primarily mediated by microglia and astrocytes (Isik et al., 2023). Under normal conditions, this response serves to protect the brain and restore its homeostasis. However, in the context of neurodegenerative diseases (ND), such as Alzheimer's disease (AD) or Parkinson's disease (PD), neuroinflammation becomes chronic and destructive, contributing to the progression of neuronal damage. Prolonged activation of glial cells results in the overproduction of pro-inflammatory cytokines, oxidative stress, and disruption of neuronal signaling (DiSabato et al., 2016).

In this context, mesenchymal stem cell (MSC)-derived exosomes (Exo) have drawn considerable interest due to their natural regenerative and immunomodulatory properties. Through the delivery of key regulatory molecules, these Exo help attenuate neuroinflammatory processes and contribute to the maintenance of neural homeostasis (Thomi et al., 2019, Peng et al., 2022).

Quercetin (Que), a natural flavonoid known for its antioxidant and anti-inflammatory effects, has shown potential in inhibiting neuroinflammation (Jembrek et al., 2021). However, its poor solubility and low bioavailability remain major limitations (Gonçalves et al., 2015). To overcome these challenges, loading quercetin into Exo may enhance its stability, improve cellular uptake, and increase its anti-inflammatory efficacy within the brain.

Based on this idea, our aim was to investigate the use of Que-loaded Exo (Que-Exo) as a therapeutic approach to mitigate neuroinflammation, which may contribute to the development of effective treatments against NDs in the future.

2. GENERAL INFORMATION

2.1. Neuroinflammation

Neuroinflammation is a response that occurs in the CNS (Shabab et al., 2017; Isik et al., 2023), involves the activation of various cells, including macroglia, microglia, and neurons. This response is triggered by a wide range of factors, such as the initial insult to the CNS, genetic predispositions, environmental influences, an individual's age, and prior experiences that may have primed the immune system.

A hallmark event in the initiation and propagation of neuroinflammation is microglial activation, the resident immune cells of the CNS (Shabab et al., 2017). This activation process involves a range of changes, including morphological alterations (Paolicelli & Gross, 2011), proliferation (Gómez-Nicola et al., 2013), and migration to the sites of injury or infection (Lively & Schlichter, 2013). These activated microglia, along with endothelial cells, peripherally derived immune cells, and other resident glial cells such as astrocytes, play a pivotal role in orchestrating the inflammatory response.

Once activated, microglia and other immune cells release a variety of mediators that are crucial in shaping the outcome of neuroinflammation. These include cytokines, which are signaling proteins that regulate the immune response; chemokines, which guide the movement of immune cells to sites of injury; reactive oxygen species (ROS), which can have both protective and damaging effects; and secondary messengers that further amplify the inflammatory signal (DiSabato et al., 2016).

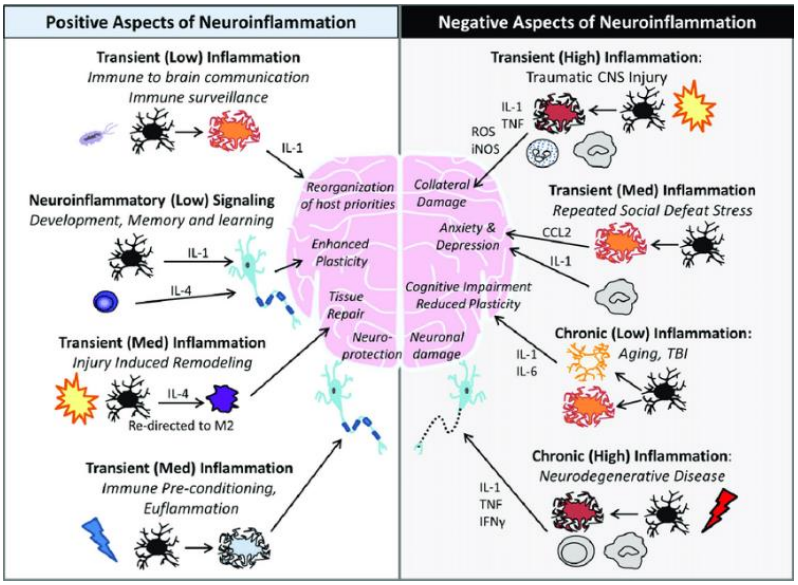

Figure 1: Positive and negative aspects of neuroinflammation (DiSabato et al., 2016).

2.2. Microglia

2.2.1. Origin and Characteristics of Microglia

Microglia are the primary immune cells residing within the CNS, playing a vital role in maintaining brain homeostasis, responding to injury, and modulating neural networks. These specialized cells constantly survey the brain environment and responding to a variety of stimuli, both pathological and physiological. Their capacity to detect and respond to changes enables microglia to serve as the first line of defense against threats such as pathogens or tissue damage. Originating from early erythroid myeloid progenitors (eEMPs) located in the yolk sac (**Figure 2**) (de Araújo et al., 2022), microglia are distinct from other immune cells and are classified as resident macrophages of the CNS (Streit et al., 2004). This unique lineage allows them to effectively contribute to immune surveillance, tissue homeostasis, and the response to injury within the brain. Moreover, microglia are distributed evenly throughout the CNS, ensuring comprehensive coverage and oversight of the neural environment (Isik et al., 2023).

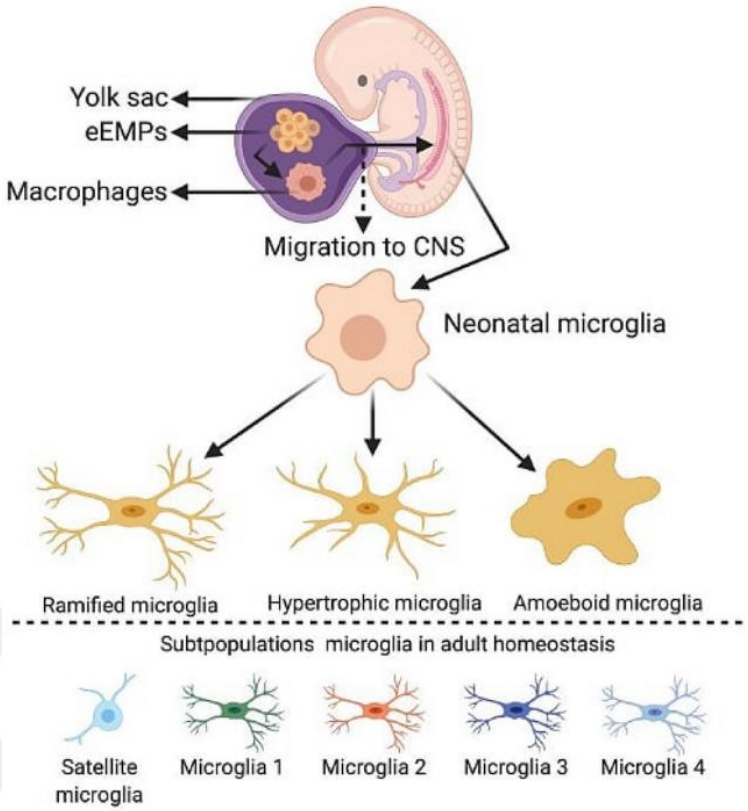

Figure 2: Origination of microglia from eEMPs in the yolk sac and their migration to brain parenchyma (de Araújo et al., 2022).

Microglia play a central role in mediating neuroinflammation (Streit et al., 2004) and are essential for maintaining tissue homeostasis, removing invading pathogens, and promoting recovery from injury (Zhang et al., 2023). Additionally, they play a major role in neurodegenerative disorders and brain inflammation (Harry & Kraft, 2012; Shabab et al., 2017).

2.2.2. Morphology of Microglia

The morphology of microglia serves as a visual indicator of their activation and functional states. In a healthy brain, microglia exhibit a ramified morphology, characterized by small cell bodies and long, thin, highly branched processes. Therefore, microglia form a complex network that permits them to interact with blood vessels, astrocytes, and neurons. This ramified form enables microglia to effectively monitor the brain microenvironment, constantly surveying for signs of disturbance or damage (Streit et al., 1999).

Nevertheless, upon microglial activation triggered by factors such as infection, trauma, or neurodegenerative processes, microglia undergo significant morphological changes. They undergo a morphological change from ramified to amoeboid (**Figure 3**), characterized by an enlarged, rounded cell body and retraction of their branched processes. This amoeboid form is associated with an escalation in the pro-inflammatory and phagocytic activities of cells (Kettenmann et al., 2011). The cytoplasm becomes enlarged, reflecting the cell's heightened capacity to engulf and digest cellular debris, pathogens, or damaged cells (Streit et al., 1999).

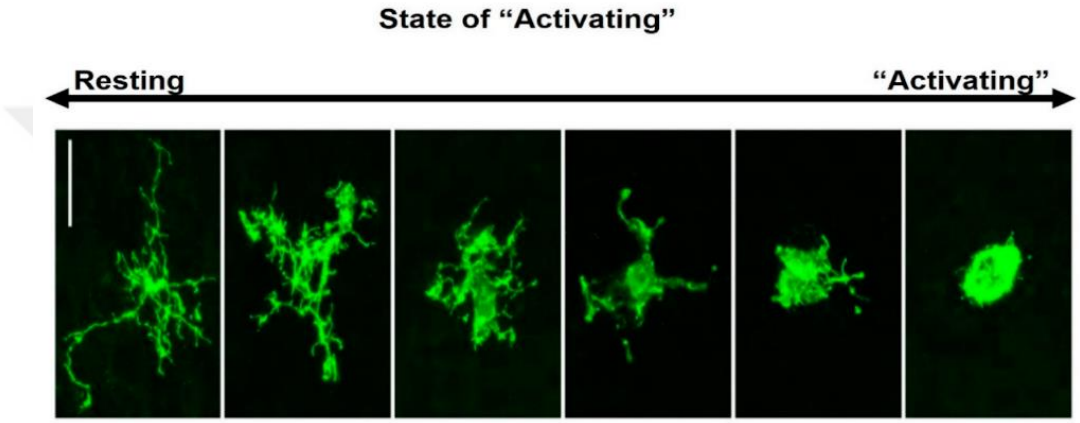

Figure 3: Distinct morphological characteristics of microglia in their ramified and amoeboid forms (Rawlinson et al., 2020).

2.2.3. Activation of Microglia

The microglia in the CNS adopt various functional phenotypes, depending on the specific conditions and signals present in their environment. They can adopt either pro-inflammatory or neuroprotective roles based on their activation state (Salvi et al., 2017). **M1 microglia** are associated with neuroinflammation and neurotoxicity and are often triggered by factors such as pathogens, tissue damage, neurotoxins, infection, or injury (Isik et al., 2023). Hence, they can physically assault healthy neurons through processes such as phagocytosis or the release of apoptotic factors (Shabab et al., 2017). In response to these triggers, microglia can undergo physiological changes that drive them into a "reactive state," during which they secrete inflammatory molecules that contribute to neuroinflammation (Isik et al., 2023).

Neuroinflammation can be either acute or chronic, and plays a significant role in CNS pathologies (Streit et al., 2004). Acute inflammation is a rapid response involved in tissue repair, typically triggered by injury or infection. In contrast, chronic inflammation is linked to NDs, which is associated with neuronal impairment, damage, and disease progression (Streit et al., 2004; Isik et al., 2023).

Upon activation, microglia engage in various activities: they gather at the site of injury, proliferate, migrate, phagocytize debris, present antigens to T cells, and release oxidative molecules. They also activate multiple genes and proteins, including pro-inflammatory enzymes such as, inducible nitric oxide synthase (iNOS), cyclooxygenase-1 (COX-1), cyclooxygenase-2 (COX-2), pro-inflammatory cytokines like interleukin-1 beta (IL-1β), tumor necrosis factor-alpha (TNF-α), and ROS. During chronic inflammation, microglia can stay in an active state for prolonged periods, persistently secreting neurotoxic factors and inflammatory cytokines, which exacerbate neurodegeneration over time.

Moreover, the nuclear factor-κB (NF-κB) signalling pathway triggers the expression of the NOD-like receptor pyrin domain-containing protein 3 (NLRP3) inflammasome. A plethora of research has shown the role of this inflammasome in modulating the release of inflammatory cytokines following microglial activation in chronic NDs (Barczuk et al., 2022). Hence, preventing the secretion of pro-inflammatory mediators induced by the activation of microglia may be a useful treatment approach for slowing the progression of NDs (Shabab et al., 2017).

For instance, systemic inflammatory response syndrome is triggered by lipopolysaccharide (LPS), a toxic component on the outer membrane of gram-negative bacteria, via toll-like receptor (TLR) signalling, as illustrated in **Figure 4**. LPS interacts with toll-like receptor 4 (TLR4) on microglial surfaces, initiating several intracellular signaling cascades, including mammalian target of rapamycin (mTOR), mitogen-activated protein kinase (MAPK), and phosphoinositide 3-kinase/protein kinase B (PI3K/AKT). In fact, these pathways ultimately result in the activation of NF-κB. Subsequently, stimulating the expression of pro-inflammatory cytokines, chemokines, and enzymes such as COX-2 and iNOS, which are key contributors to the neuroinflammatory response (Shabab et al., 2017). Such inflammation influences not

only immune functions but also physiological, metabolic, and psychological states. Furthermore, the length and progression of the initial stimulation determine the extent of neuroinflammation (DiSabato et al., 2016).

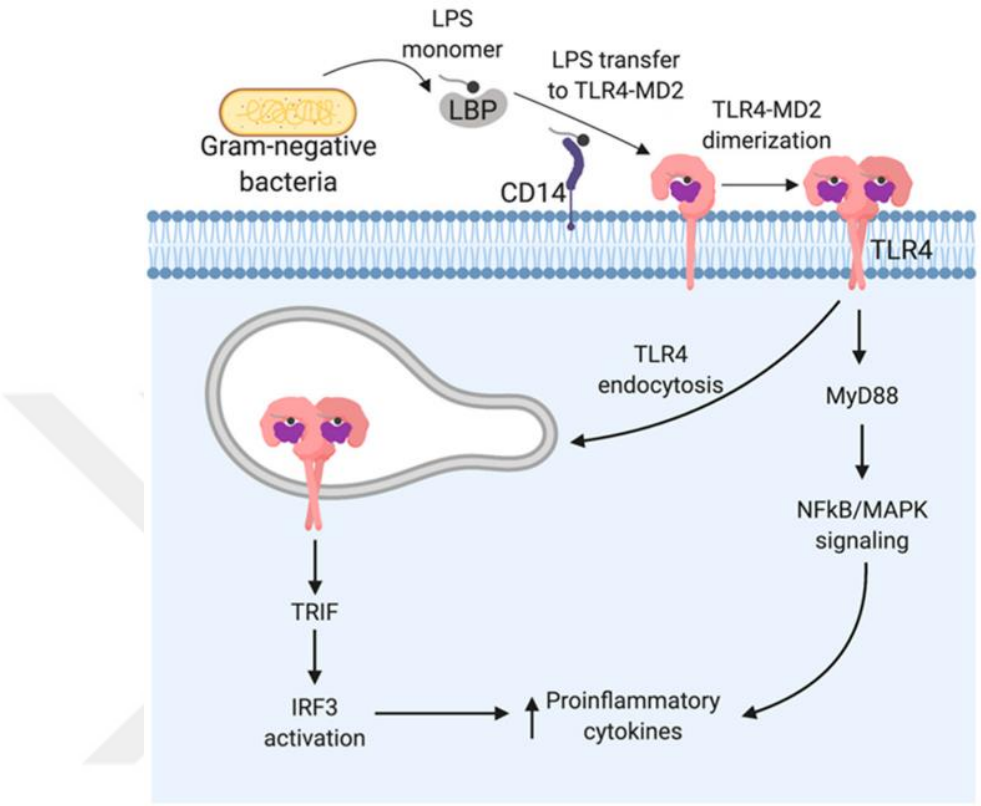

Figure 4: Initiation of LPS-mediated neuroinflammation (Mazgaeen et al., 2020).

Conversely, the activation of **M2 microglia**, termed "alternative activation," is triggered by anti-inflammatory signals including IL-4, IL-10, IL-13, TGF-β, and glucocorticoids. This activation state is essential for resolving inflammation and promoting the re-establishment of homeostasis within the CNS. M2 microglia are distinguished by surface markers like the mannose receptor (CD206) and Triggering receptor expressed on myeloid cells 2 (TREM2), which are integral to their anti-inflammatory function. Furthermore, these cells release anti-inflammatory and tissue-repair-related factors such as arginase-1 (Arg-1), which supports extracellular matrix formation and healing processes. They also produce growth factors including insulin-like growth factor 1 (IGF-1), chitinase 3-like 3 (Ym-1), and found in inflammatory zone 1 (FIZZ1), which aid in matrix remodeling and tissue regeneration (Salvi et al., 2017).

The distinct functions of the M1 and M2 microglial phenotypes in both inflammatory responses and homeostatic maintenance are illustrated in **Figure 5**.

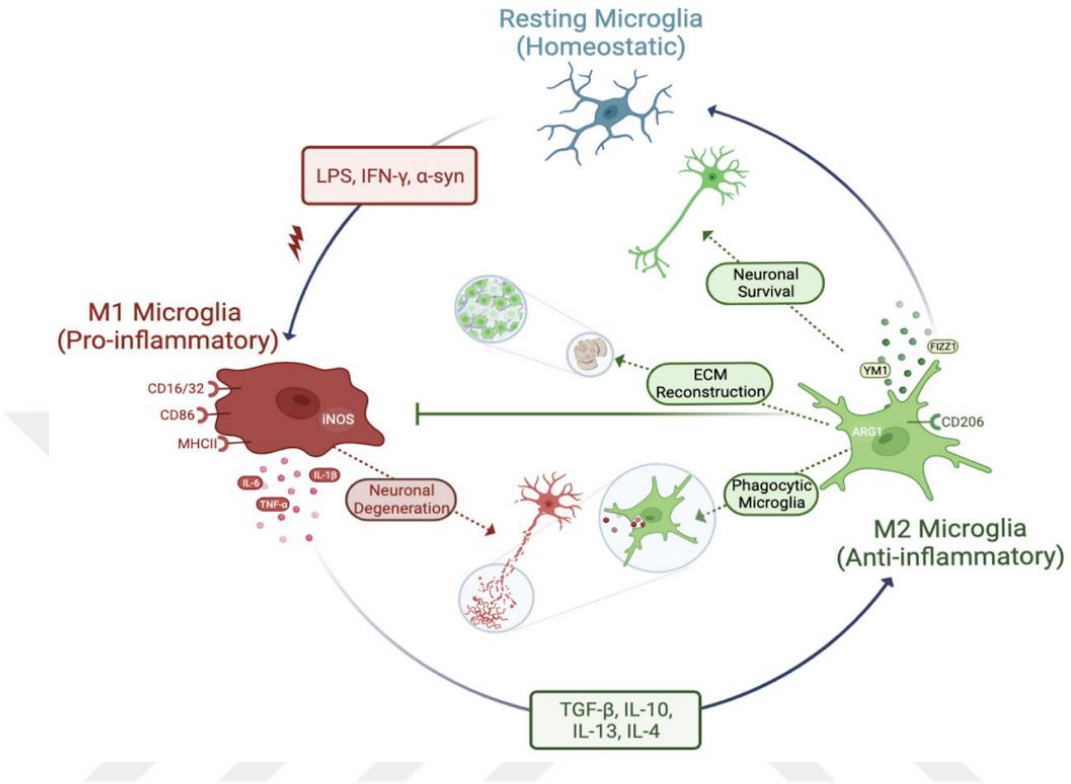

Figure 5: M1 and M2 microglia phenotypes (Isik et al., 2023).

2.2.4. HMC3 Cell Line

Although microglial activation and functions have been extensively studied in *in vivo* models, research utilizing human microglia remains limited, primarily due to the difficulty in obtaining primary human microglial cells. To overcome this limitation, several immortalized human microglial cell lines have been established (Dello Russo et al., 2018).

One such line is HMC3 (Human Microglia Clone 3), which originates from fetal brain tissue and was immortalized using the SV40 large T antigen. This modification enables the cells to proliferate continuously *in vitro* while preserving many of the essential characteristics of primary human microglia (Gunasegaran et al., 2025). HMC3 cells display diverse and complex morphology, including vacuolated cytoplasm and short cellular extensions. Additionally, they express key myeloid markers such as

CD68, CD11b, and CD14 (Dello Russo et al., 2018).

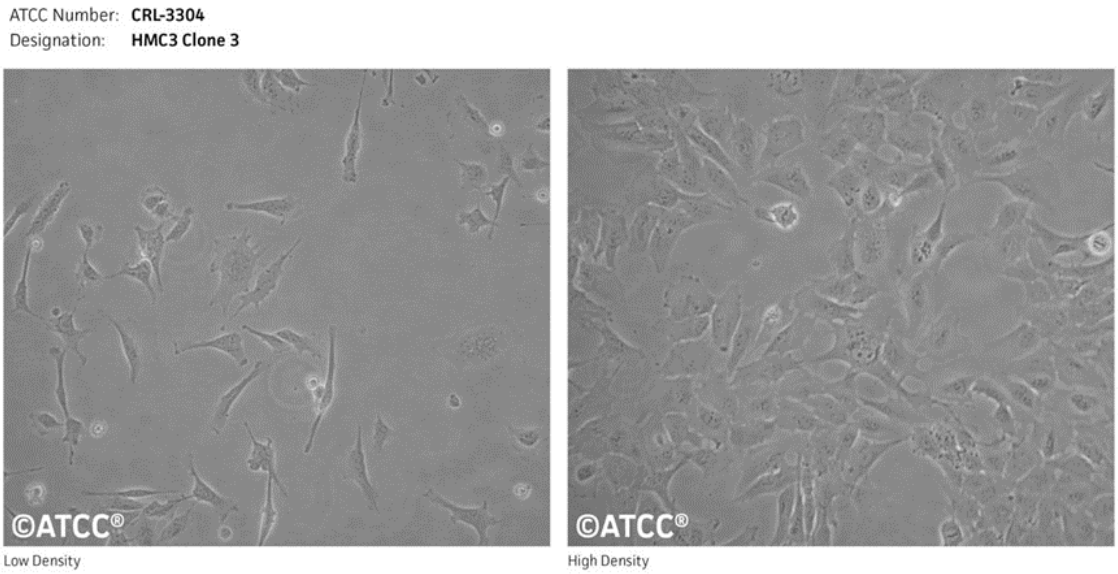

Figure 6: Morphology of HMC3 (ATCC CRL-3304).

The HMC3 cell line is extensively used in neuroinflammation research, serving as a reliable model for studying microglial activation and behaviour under diverse stimuli (Etemad et al., 2012; Li et al., 2018).

2.3. Stem Cells

Stem cells are the building blocks of every cell in the body and have a tremendous potential to ameliorate human health (Weissman et al., 2000). These undifferentiated cells possess the ability to self-renew and differentiate into various specialized cells within an organism. Mesenchymal stem cells (MSCs), which can be isolated from multiple tissues, have the capacity to develop into bone, cartilage, and adipose cells (Zakrzewski et al., 2019). Due to their unique immunological properties, ease of laboratory cultivation, and ability to differentiate into diverse cell lineages, MSCs are considered highly valuable for cell-based therapies and tissue repair strategies (Abbaszadeh et al., 2020).

2.3.1. Umbilical Cord-Derived Mesenchymal Stem Cells

The umbilical cord (UC) joins the placenta and fetus to enable gas exchange (oxygen and carbon dioxide) and feeding. It is composed of two main parts: the perivascular region, which surrounds and protects the blood vessels, and the central portion called Wharton's jelly (WJ). The WJ is abundant in glycosaminoglycans such as hyaluronic acid and chondroitin sulfate, giving the cord its gelatinous structure and elasticity. UC collection is non-invasive and does not raise any moral concerns, making it an attractive source for obtaining large numbers of MSCs (Halbutoğulları et al., 2023). MSCs obtained from WJ of the UC (UC-MSCs) show promising potential for future clinical applications. They are appealing because of their limited variability and unique characteristics, including straightforward isolation and culture, widespread presence in tissues, immunomodulatory effects, self-renewal capability, multipotent differentiation, and lack of ethical concerns. Moreover, the process of obtaining and isolating UC-MSCs avoids invasive surgical procedures, ensuring that there are no complications or risks for the donor. This provides an advantage over other MSC sources.

2.3.2. Limitations of Mesenchymal Stem Cells

In the application of stem cell-based therapies, it is crucial to carefully consider possible opposing effects. One concern is tumorigenesis, which may occur following stem cell transplantation due to their prolonged proliferative capacity and resistance to apoptosis. In addition, MSCs tend to have low engraftment because of their limited viability shortly after the injection. Although most research indicates that a single MSC transplant is generally safe and does not provoke an immune response, repeated MSC injections can potentially induce the formation of allo-antibodies (Abbaszadeh et al., 2020). Moreover, MSCs express major Histocompatibility Complex (MHC) class I, which may strongly stimulate allogeneic immune responses that cause tissue damage and inflammation in recipients (Harrell et al., 2021). Consequently, it is essential to employ a distinct yet advantageous method to ensure the long-term treatment of neuroinflammation. These limitations can be overcome by employing alternative methods aimed at reducing neuroinflammation and enhancing neuroregeneration.

2.4. Exosomes

2.4.1 Characteristics and Compositions of Exosomes

Cells produce exosomes (Exo), which are membrane-containing vesicles, where their sizes range between 30–150 nm (Doyle & Wang, 2019). They can perform essential tasks such as preserving cellular homeostasis, eliminating cellular trash, and promoting intercellular communication by delivering biochemical such as proteins, lipids, mRNA, miRNA, and DNA (He et al., 2023; Krylova & Feng, 2023) (**Figure 7**). The lipid bilayer membrane that encloses Exo is made up of phosphatidylserine, phosphatidylcholine, sphingomyelin, ceramides, and cholesterol, which is vital for preserving both their stability and activity (Kalluri et al., 2020).

Exo are enriched with a wide variety of proteins located on their membranes as well as within their cytosol. Proteins involved in membrane transport and fusion are particularly abundant, enabling Exo to interact with recipient cells effectively. On their surface, Exo are densely packed with proteins that bind to receptors on target cells, triggering intracellular signalling pathways. They also display surface glycoproteins, glycolipids, and various signalling agents like cytokines, growth factors, small molecules, and metabolites. Furthermore, they are capable of transporting various bioactive substances, including proteins, metabolites, and nucleic acids (Kalluri et al., 2020). This diverse molecular composition underscores their potential in intercellular communication and their emerging potential in therapeutic applications (Dixson et al., 2023).

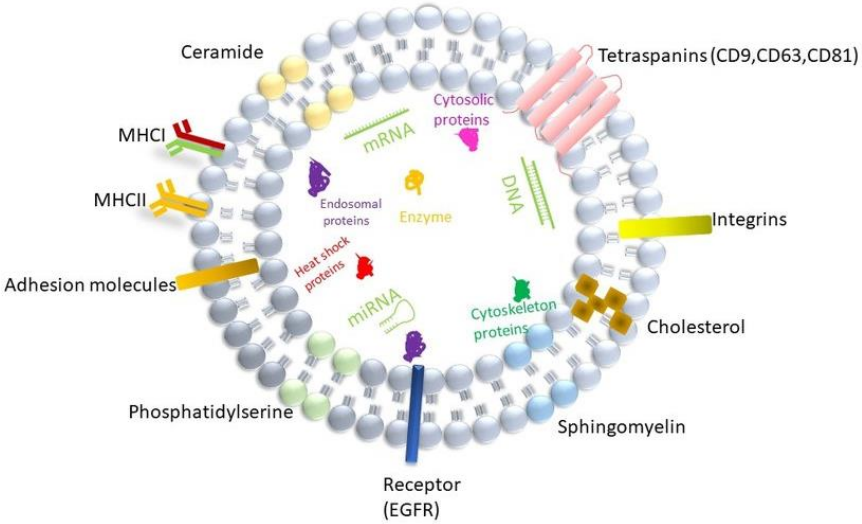

Figure 7: Structure and composition of exosome (Xiao et al., 2021).

Exo have attracted considerable interest owing to their distinct features that set them apart from other types of extracellular vesicles (EVs). Specifically, their distinct compositions and roles in intercellular communication have made them a central focus of research, with profound implications for understanding pathophysiological processes and advancing innovative therapeutic approaches (Kalluri et al., 2020) (**Figure 8**).

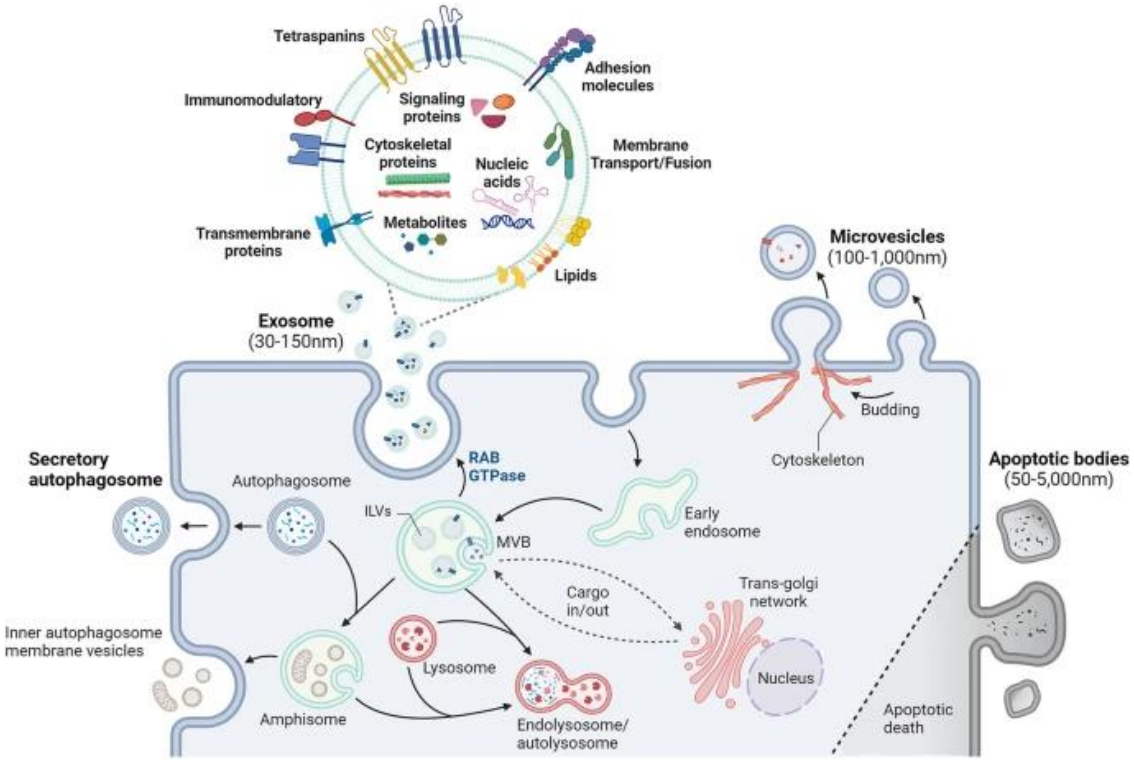

Figure 8: Multiple pathways of EV Biogenesis (Lee et al., 2024).

Moreover, Exo transport their molecular messages, known as "cargo" (He et al., 2023), via autocrine, paracrine, and endocrine pathways, circulating through all bodily fluids (Krylova & Feng, 2023). The cargo can be present either on the surface or within the Exo. Externally, cargo components can directly interact with recipient cells, triggering signalling pathways or facilitating targeted delivery. Internally, cargo is released once the Exo is taken up by recipient cells, subsequently modulating cellular processes at the genetic, protein, or lipid levels. The presence of both surface-bound and internal molecular components enhances the versatility of exosomes in facilitating intercellular communication and the transfer of biological information. Therefore, the precise sorting and encapsulation of specific biomolecules during exosome formation

are fundamental to their development and functionality. Gaining insights into the molecular mechanisms governing cargo selection during exosome biogenesis is critical for understanding their physiological significance and holds great promise for the development of innovative diagnostic and therapeutic applications across a wide range of diseases (Lee et al., 2024).

2.4.2. Biogenesis of Exosomes

The processes of biogenesis and secretion for Exo are distinct from those of microvesicles. Microvesicles are generated through the outward budding of the plasma membrane, while Exo are released through the fusion of multivesicular bodies (MVBs) with the plasma membrane (**Figure 9**) (Rastogi et al., 2021). Research has shown that Exo formation is highly dependent on the physiological states of both donor and recipient cells, resulting in differences in the protein, lipid, and nucleic acid compositions of various Exo (Pegtel et al., 2019).

Exo formation initiates with the Golgi apparatus releasing cargo, which is then directed to endosomal membranes that evolve into MVBs, generally ranging from 250 to 1000 nm in diameter. As MVBs mature, numerous intraluminal vesicles (ILVs) develop, measuring between 30 and 150 nm, via inward invagination of the endosomal membrane (Heijnen et al., 1999). During this maturation phase, particular cargoes are sorted and integrated into ILVs through selective pathways, which encompass both **ESCRT-dependent** and **ESCRT-independent** mechanisms (**Figure 10**) (Henne et al., 2011; Stuffers et al., 2009).

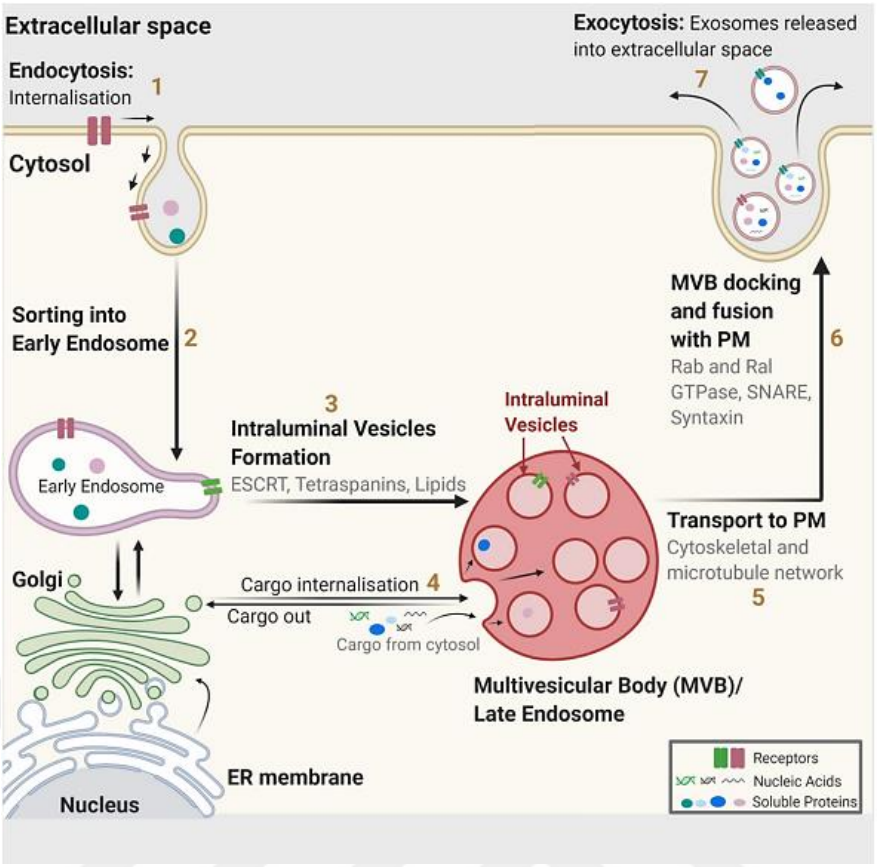

Figure 9: The mechanism of exosome's biogenesis (Gurung et al., 2021).

The **ESCRT-dependent pathway** involves a conserved set of protein complexes, namely ESCRT-0, ESCRT-I, ESCRT-II, and ESCRT-III—that are are essential for cargo selection and the formation of MVBs and ILVs. In fact, ESCRT-0 and ESCRT-I are responsible for the segregation of ubiquitinated cargo into lipid microdomains located on the membranes of MVBs, whereas ESCRT-II and ESCRT-III facilitate the invagination process and the subsequent formation of MVBs and ILVs. Additionally, other proteins, including ALG-2-interacting protein X (ALIX), tumor susceptibility gene 101, and vacuolar protein sorting-associated protein (VPS4), contribute to this pathway (Rastogi et al., 2021).

Nevertheless, the **ESCRT-independent pathway** employs tetraspanin clusters of differentiation like CD63, CD81, CD82, CD37, and CD9, along with molecular chaperones like HSP60, HSP70, and HSP90, to aggregate cargo within lipid microdomains, facilitating the formation of MVBs and ILVs (Colombo et al., 2019; Lötvall et al., 2014; Mulcahy et al., 2014). CD63 and CD81 are commonly found on ILV membranes and serve as exosome markers. Additionally, syntenin contributes to

the ESCRT-related sorting and recycling of cargo during vesicle formation (Rastogi et al., 2021).

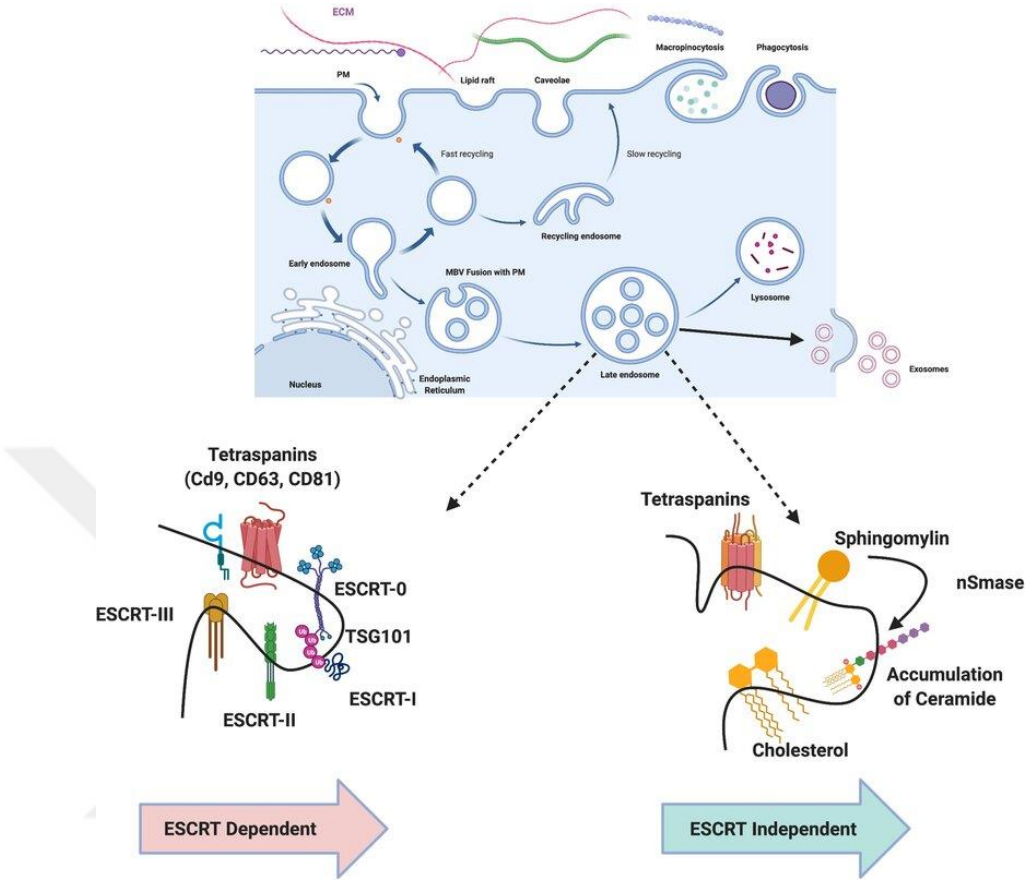

Figure 10: Biogenesis of exosomes by ESCRT dependent and independent pathways (Gurunathan et al., 2021).

Exo biogenesis is influenced by both ESCRT-dependent and independent mechanisms, with the choice of pathway primarily determined by the specific cargo and the type of cell involved (Mulcahy et al., 2014). The transfer and docking of MVBs to the plasma membrane are energetically supported by Ras-associated binding (Rab) GTPases. The subsequent fusion of MVBs with the plasma membrane requires the action of soluble NSF attachment protein receptor (SNARE) complexes (Anand et al., 2019; Klumperman et al., 2014; Stuffers et al., 2009). Once fusion occurs, MVBs release their ILVs, which transform into Exo as they enter the extracellular environment. However, it is important to recognize that not all MVBs proceed to

exocytosis; some are redirected to lysosomes for degradation instea (Rastogi et al., 2021).

2.4.3. Exosome Interactions with Recipient Cell

Upon arriving at the target cell, Exo can initiate signalling by binding directly to extracellular receptors, fusing with the plasma membrane, or being internalised by the cell (Gurung et al., 2021).

Direct Interaction: Ligands present on Exo can engage with receptors on target cells, initiating a series of intracellular signalling pathways. This interaction is essential for modulating immune responses and inducing cell apoptosis. For instance, Exo secreted from dendritic cells activate T lymphocytes through MHC-peptide complexes (Tkach et al., 2017) and engage TLRs on bacterial cells, thereby activating nearby dendritic cells and boosting immune responses (Sobo-Vujanovic et al., 2014). Exo derived from UC blood, which display tumor antigens like MHC-I and MHC-II, and tetraspanins CD34 and CD80 (Guan et al., 2014), facilitate T cell proliferation and support antitumor responses. Ligands such as TNF, Fas ligand (Fas), and TNF-related apoptosis-inducing ligand (TRAIL) on Exo surfaces can bind to TNF receptors on tumor cells, triggering caspase activation and leading to apoptosis (Munich et al., 2012).

Fusion with Plasma Membrane: Exo can also fuse directly with the plasma membrane of recipient cells, allowing their contents to enter the cytosol. This fusion process is thought to be aided by SNARE and Rab protein families, which play roles similar to those involved in cell membrane fusion (Gurung et al., 2021). Moreover, lipid raft-like domains, along with integrins and adhesion molecules on Exo surfaces, help facilitate these interactions and the fusion process with recipient cells (Mulcahy et al., 2014, Valapala et al., 2011).

Internalisation: Exo are internalised by target cells, leading to the release of their cargo into the cytoplasm (Joshi et al., 2020; Tian et al., 2014). This uptake is a fast, temperature-dependent process, where colder conditions reduce the rate of internalisation (Escrevente et al., 2011).

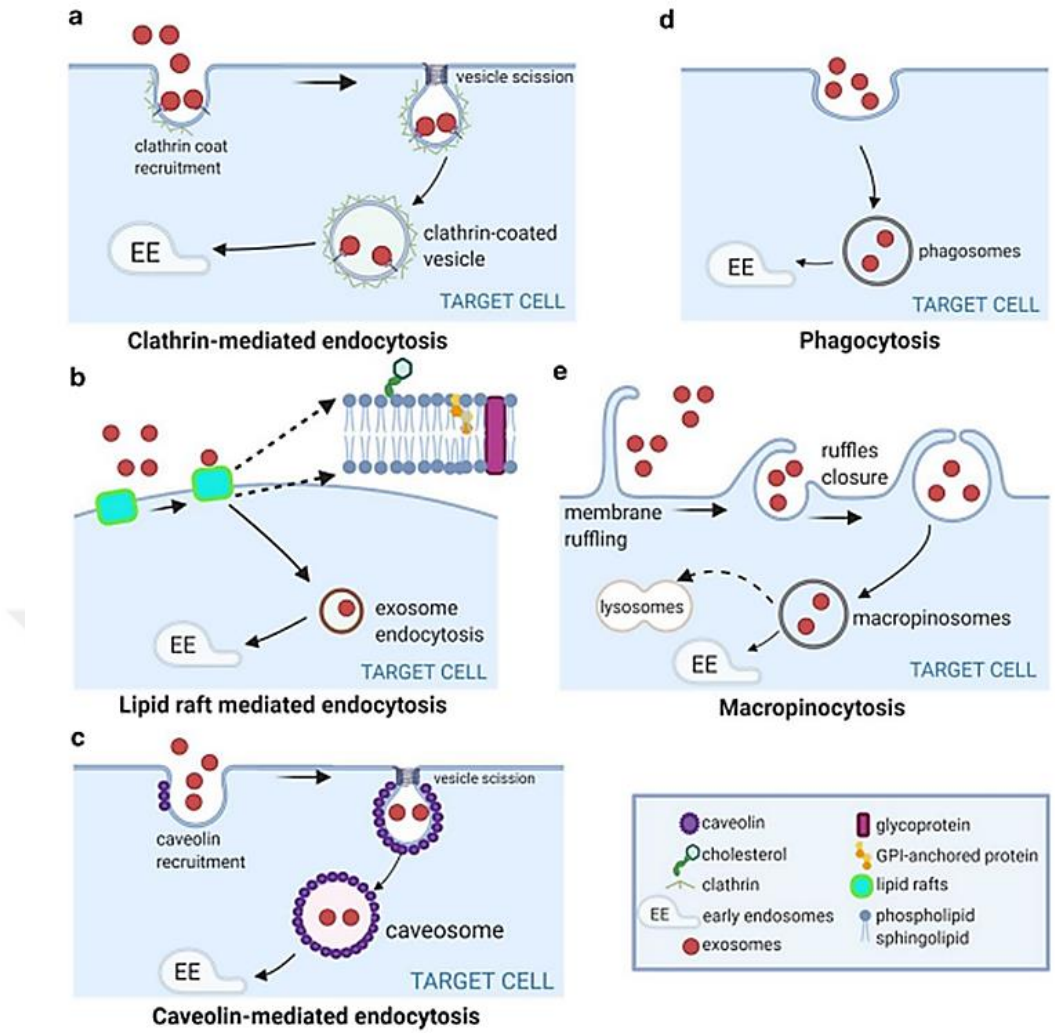

Figure 11: Different exosome internalisation pathways (Gurung et al., 2021).

Exo entry commonly occurs through many endocytic pathways (**Figure 11**), notably **clathrin-mediated endocytosis**. During this process, receptors and ligands accumulate progressively, forming clathrin-coated vesicles that, once internalised, shed their coats and merge with endosomes (Mettlen et al., 2018). This uptake mechanism is observed across various cells like ovarian and colon cancer cells (Escrevente et al., 2011; Verweij et al., 2018), cardiomyocytes (Eguchi et al., 2019), macrophages (Benmerah et al., 1999; Feng et al., 2010), hepatocytes (Benmerah et al., 1999), neural cells (Guan et al., 2014), and epithelial cells (Yoon et al., 2020), highlighting its dependence on clathrin-mediated components. The inhibition protein dynamin-2 has been demonstrated to reduce Exo uptake in macrophages (Barrès et al., 2010; Feng et al., 2010) and microglial cells (Fitzner et al., 2011). Furthermore, the transferrin

receptor's overexpression boosts Exo uptake by cancer cells, suggesting clathrin-mediated endocytosis is a main route for Exo internalisation (Amber Gonda et al., 2019).

Another key endocytic pathway is **lipid raft-associated membrane invagination**, which facilitates the transfer of cargo into early endosomes and impacts Exo uptake (Delenclos et al., 2017). Lipid rafts are stable microdomains enriched with cholesterol, sphingolipids, and GPI-anchored proteins (Mulcahy et al., 2014). Changes in lipid metabolism can disrupt Exo uptake; for instance, using agents like methyl-β-cyclodextrin reduces Exo uptake in breast cancer cells (Koumangoye et al., 2011). Likewise, inhibiting sphingolipid synthesis impairs Exo uptake in dendritic cells, and disruptions in cholesterol transport further hinder this process. Calcium-regulated membrane-binding protein (ANXA2) enhances this pathway by anchoring Exo to specific adhesion sites on the cell surface. Additionally, flotillin, a protein associated with lipid rafts, plays a supportive role in promoting lipid type of endocytosis (Gurung et al., 2021).

Caveolin-dependent endocytosis involves caveolin, an integral membrane protein, which creates small invaginations on the plasma membrane. These caveolae support the internalisation of caveosomes, which are larger vesicles containing hydrophobic lipids. In fact, caveolin-1, 2, and 3 make up the caveolae (Kiss et al., 2009). In epithelial cells, Caveolin-1 has been demonstrated to promote Exo uptake (Nanbo et al., 2013), though it can reduce uptake in fibroblasts and glioma cells (Svensson et al., 2013).

Exo uptake can also occur through **phagocytosis**, a process where immune cells internalise large particles and, occasionally, smaller ones like Exo, forming phagosomes that ultimately transport the internalised cargo to lysosomes for degradation (Gordon et al., 2016). This process relies on the closure of phagosomes, with enzymes such as PI3K and phospholipase C (PLC) playing essential roles (Fukami et al., 2010).

Macropinocytosis is characterised by inward folding of the plasma membrane, driven by actin, resulting in the formation of macropinosomes. This pathway relies on growth factors for uptaking extracellular molecules (Lim et al., 2011). This process can

be influenced by several regulatory factors, including Rac1 GTPase and Na+/H+ exchanger activity (Kerr et al., 2009).

Additionally, there has been recent identification of a specific filopodial entry route in fibroblasts (Heusermann et al., 2016). Filopodia are actin-rich protrusions that help cells interact with their environment (Mattila et al., 2008), and they can also influence processes such as Exo uptake, resembling how pathogenic bacteria and viruses enter cells (Lehmann et al., 2005). Exo can travel along filopodia before being internalised, sometimes through pulling motions. Nevertheless, additional work is required to ascertain the particulars of this process and its exclusivity to fibroblasts. (Gurung et al., 2021).

2.4.4. Advantages of Exosomes

Exo offer numerous advantages, making them valuable in diagnostics, research, and therapeutics. As natural drug delivery vehicles, they are biocompatible and non-immunogenic (Rajput et al., 2022), able to deliver both hydrophilic and hydrophobic molecules. The high stability of Exo (Nikfarjam et al., 2020) allows them to easily pass across a variety of physiological barriers, such as plasma membrane of cells and the blood-brain (BBB). In addition, their lipid bilayer structure permit them to fuse with other membrane-like bodily structures, notably the BBB (He et al., 2023). Furthermore, Exo are involved in a wide range of cell-to-cell communication pathways that are connected to both physiological and pathological processes (Nikfarjam et al., 2020). They are also a type of biological machinery that can be dysregulated or captured by pathogenic processes in many disease situations. This phenomenon has sparked heightened interest in investigating Exo as potential diagnostic markers and therapeutic targets (Krylova & Feng, 2023). They have also demonstrated great promise as alternatives to cellular treatments (Halbutoğulları et al., 2023). They are also ideal for non-invasive diagnostics, as they can be isolated from body fluids like blood, urine, and saliva, with their molecular cargo reflecting the originating cells' physiological or pathological state (Kanninen et al., 2016). Hence, their natural origin reduces toxicity and minimises off-target effects, positioning Exo as a powerful and versatile tool in advancing personalised medicine and innovative therapeutic strategies (Rajput et al., 2022).

2.4.5. Mesenchymal Stem Cell-Derived Exosomes

MSC-derived Exo exhibit no significant differences in morphology, isolation methods, or storage conditions compared to Exo from other sources (Fakouri et al., 2024). For identification, they express standard exosomal surface markers such as CD9 and CD81, along with adhesion molecules like CD29, CD44, and CD73, which are characteristic of the MSC membrane (Yu et al., 2014). Similar to Exo from other origins, the protein content of MSC-derived Exo varies depending on the MSC batch from which they are isolated. Functional clustering of these proteins indicates that Exo support a wide range of biological processes, aligning with the documented therapeutic efficacy of MSCs in treating various medical conditions (Fakouri et al., 2024). For instance, MSC-derived Exo are rich in various proteasome subunits, particularly the 20S proteasome. These subunits play a critical role in degrading misfolded or damaged proteins, which are essential for maintaining cellular health (Lai et al., 2012).

These Exo are enriched with microRNAs, particularly miR-133b. Research has demonstrated that this specific microRNA can significantly promote recovery in neurons and astrocytes under adverse conditions, such as those associated with Parkinson's disease. The elevated levels of miR-133b can exert a protective impact on neurons, fostering the development of nerve axons and mitigating the progression of neurodegenerative conditions. Moreover, miR-133b facilitates neurite outgrowth by modulating the extracellular Signal-Regulated Kinase 1 and 2 (ERK1/2) and PI3K/Akt signalling pathways through the inhibition of the ras homolog gene family member A (RhoA). This highlights the possible of MSC-derived Exo as a promising avenue in regenerative medicine and the advancement of novel therapeutic approaches for NDs (Peng et al., 2022).

Furthermore, MSC-derived Exo have been demonstrated to suppress microglial activation (**Figure 12**). A previous study demonstrated that Exo derived from WJ-MSCs declined pro-inflammatory cytokines secreted by the microglia BV-2 cell line and primary mixed glial cells. A considerable decrease was observed in the expression of genes LPS-induced neuroinflammation in BV-2 microglia and primary mixed glial cells. Furthermore, Exo altered BV-2 microglia's TLR4 signalling, inhibiting the phosphorylation of members of the mitogen-activated protein kinase family in response

to LPS stimulation and the degradation of the NF-κB inhibitor, known as NF-κB inhibitor alpha (IκBα). Ultimately, Exo administered intravenously to rats diminished neuroinflammation caused by microglia with perinatal brain damage (Thomi et al., 2019).

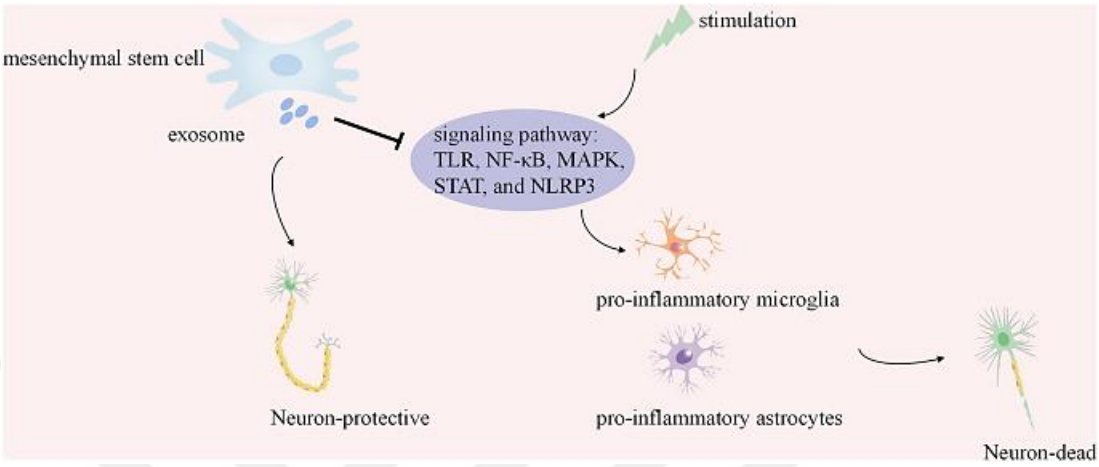

Figure 12: Mesenchymal stem cell-derived exosomes exhibit neuroprotective effects by regulating signalling pathways and attenuating neuroinflammation induced by glial cells (Ge et al., 2024).

2.5. Quercetin

Quercetin (Que; 3,3′,4′,5,7-pentahydroxyflavone) is a natural flavonoid with anti-inflammatory, anti-oxidative, and anti-apoptotic properties. It is widely found in regular meals, mostly in fruits and vegetables. The chemical structure of Que is depicted in **Figure 13**.

Due to its numerous pharmacological and health-promoting benefits, Que has been linked to promising therapeutic potential in multiple studies. Que has been demonstated to exhibit neuroprotective properties in both *in vitro* and *in vivo* models of neurodegenerative disorders. Apart from diminishing oxidative stress and neuroinflammation, Que promotes neuronal renewal and neurogenesis, while improving the functionality of preexisting neurons (Jembrek et al., 2021).

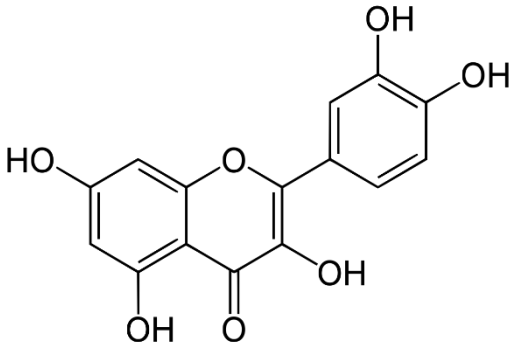

Figure 13: Chemical structure of quercetin (Salehi vd., 2020).

Moreover, Que can autofluoresce by exhibiting a particular fluorescence (488 nmex/500-540 nmem), and this phenomenon is attributed to non-covalent binding to intracellular molecules (Nifli et al., 2007). Its autofluorescence capacity allows for further examination of its cellular distribution (Pawlikowska-Pawlega et al., 2007). Que is known for its potent antioxidant and anti-inflammatory properties (Han et al., 2021); however, multiple factors, including poor water solubility, limit its bioavailability, limited absorption in the gastrointestinal tract, and rapid metabolism and excretion from the body (Gonçalves et al., 2015).

Earlier research has shown that microglial activation is mediated by both elevated ROS stress and reduced autophagy (Han et al., 2021). Moreoever, Que has been shown to modulate signalling pathways linked with neuroinflammation (Chiang et al., 2023). Que was shown to elevate Bcl-2 (B-cell lymphoma 2) and reduce Bax (Bcl-2-associated X protein) expressions, consequently inhibiting the caspase signalling and reducing p53 expression (Tumor protein P53). Hence, the antioxidant effects of Que are crucial in suppressing apoptosis. It was also demonstrated the anti-inflammatory and neuroprotective effects of Que on increasing NAD-dependent deacetylase sirtuin-1 (SIRT1) expression (Jembrek et al., 2021) by supressing the expression of NF-κB, thus decreasing the expression of the pro-inflammatory cytokines TNF-α, IL-1β, and IL-6 (Cui et al., 2022). Moreover, this powerful antioxidant reduced neuroinflammatory markers, such as iNOS and COX-2, and escalated nuclear factor E2-related factor 2 (Nrf2) and heme oxygenase-1 (HO-1) (Jembrek et al., 2021). Additionally, Que activates AMPK (AMP-activated protein kinase), which eventually induces anti-inflammatory responses (Benameur et al., 2021). **Figure 14** demonstrates the

neuroprotective effects of Que through the regulation of different intracellular signalling pathways.

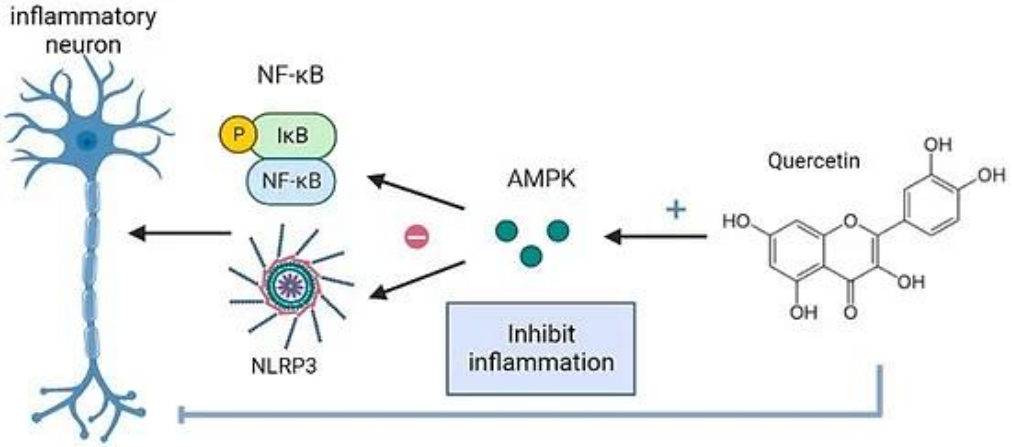

Figure 14: Neuroprotective mechanisms of quercetin (Chiang et al., 2023).

In previous research, Que was shown to dramatically reduce LPS-induced production of inflammatory mediators, microglial proliferation, and activation of the NF-κB signaling pathway. Furthermore, Que reduced the amounts of proteins associated with pyroptosis, including NLRP3 inflammasome, cleaved IL-1β, active caspase-1, GSDMD N-terminus, and the NLR family (Han et al., 2021). More recently, Que was demonstrated to dramatically reduce both NO and iNOS expressions in LPS-induced BV2 microglial cells, an effect attributed to its ability to supress NF-κB activation by stabilizing IκBα and preventing its degradation (Kang et al., 2013).

3. MATERIALS & METHODS

1. **Assessment of Quercetin's Cytotoxicity in HMC3 Cells:**

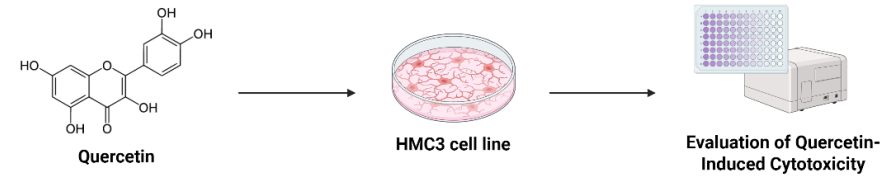

2. **Exosome Isolation & Characterization:**

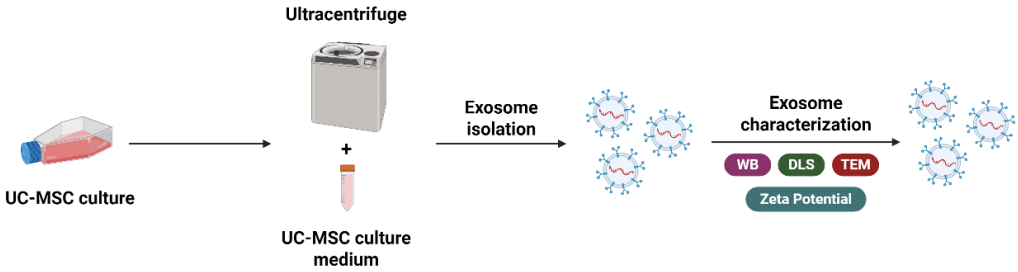

3. **Quercetin Loading into Exosomes, Characterization, Loading Efficiency, and Release Study:**

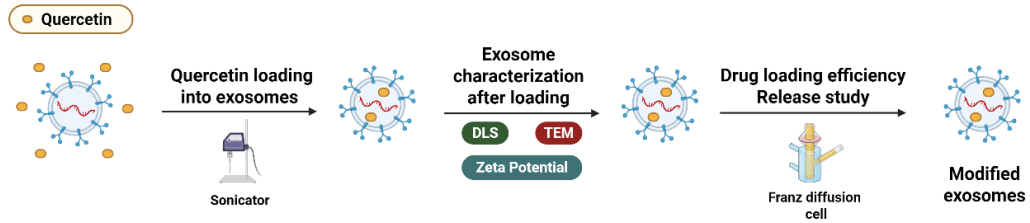

4. **Exosome Labelling and Tracking:**

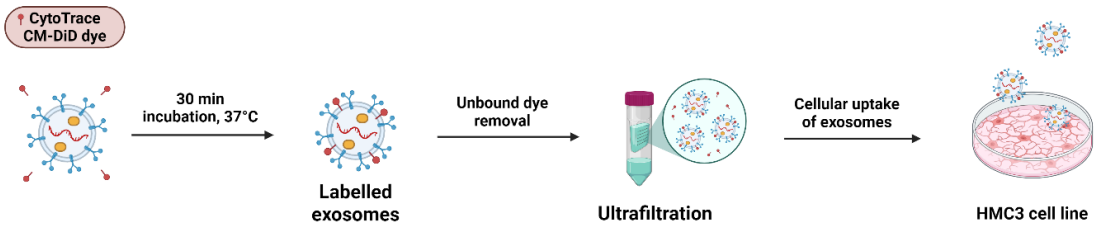

5. **Application of Modified Exosomes and Their Molecular Analysis:**

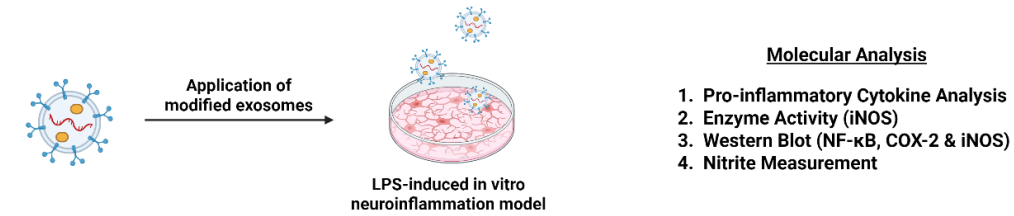

Figure 15: Overview of the Project Design.

3.1. HMC3 Cell Line Culture

3.1.1. Freezing of HMC3 Cells

To preserve HMC3 cells for a long time, they were homogenized in FBS (fetal bovine serum, Gibco, 10270106) at a density of 0.5-1 x 10^6 cells/mL. After 900µL of homogenized cells was added to each cryovial tube, they were placed on ice. Afterwards, 100 µL of DMSO (Dimethyl Sulfoxide, GENAXXON, M6323.0100) was added to each tube. Following these steps, the tubes were kept at -20ºC for 2h and then at -80ºC overnight. Finally, the tubes were transferred to a liquid nitrogen tank at -196ºC for long-term storage.

3.1.2. Thawing of HMC3 Cells

The HMC3 cells were thawed for use in future experiments. To thaw HMC3 cells, 9 mL of MEM with Earle's Salts without L-Glutamine (Minimum Essential Medium, Capricorn, MEM-XA) containing 1% pen/strep (Penicillin/Streptomycin, Capricorn, PS-B) was warmed in a 37ºC water bath and then added to a 15 mL centrifuge tube. After the cryovial tube was removed from the nitrogen tank, it was thawed in a 37ºC water bath for a maximum of 2 min. The cells were then transferred to a centrifuge tube containing MEM and centrifuged for 5 min at 1700 rpm. Subsequently, the supernatant was discarded, and the washing step was repeated to ensure complete removal of DMSO. The pellet was resuspended in complete MEM containing 15% FBS, 1% sodium pyruvate (Capricorn, NPY.B), and 1% L-glutamine (Capricorn, GLN.B), and then seeded in a 25 cm^2 flask. Later, the cells were incubated at 37ºC in a humidified atmosphere with 5% CO_2.

3.1.3. Subculture of HMC3 Cells

The human Microglial HMC3 cell line was purchased from the American Type Culture Collection (ATCC, USA, CRL-3304) within the scope of the previously accepted TÜBİTAK 1001 project. Cells were seeded in MEM with Earle's Salts without L-glutamine, containing 10% FBS, 1% sodium pyruvate, 1% L-glutamine, and 1% pen/strep. When the cells reached 70-80% confluency, cell passaging was performed. The old medium was discarded from the flask, followed by washing with 3 mL PBS. Afterwards, adherent cells were detached from the flask using 1 mL of 0.25%

Trypsin-EDTA solution and kept in an incubator at 37ºC for 2 min. The cells were observed under a microscope (Zeiss, Zen 3.3) to ensure detachment from the flask surface. Deactivation of trypsin was performed after adding 3 mL of 10% FBS-contained MEM, then the cells were transferred to a 15 mL centrifuge tube and centrifuged at 1700 rpm for 5 min. Subsequently, the supernatant was discarded, and the pellet was homogenized in 1 mL of complete MEM. For cell counting, 20 µL of suspended cells were mixed with the same amount of Trypan blue and added on both sides of a hemocytometer. After performing the calculations, 5 x 10^4 cells were seeded in a 25 cm^2 flask containing complete MEM as previously optimized and then incubated at 37ºC in a humidified atmosphere with 5% CO_2. The medium was refreshed every day, and the cells were subcultured twice per week.

3.2. UC-MSC Culture

3.2.1. Freezing of UC-MSC

To preserve UC-MSCs for a long time, they were homogenized in MSC-qualified FBS (fetal bovine serum, Gibco, 10270106). After 900µL of homogenized cells was added to each cryovial tube, they were placed on ice. Afterwards, 100µL of DMSO (Dimethyl Sulfoxide, GENAXXON, M6323.0100) was added to each tube. Subsequently, the tubes were kept at -20ºC for 2h and then at -80ºC overnight. Finally, the tubes were transferred to a liquid nitrogen tank at -196ºC for long-term storage.

3.2.2. Thawing of UC-MSC

The UC-MSCs were thawed for use in future experiments. To thaw UC-MSCs, 15 mL of DMEM-LG (Dulbecco's Modified Eagle Medium-Low Glucose, Gibco) containing 1% pen/strep was warmed in a 37ºC water bath and then added to a 15 mL centrifuge tube. After the cryovial tube was removed from the nitrogen tank, it was thawed in a 37ºC water bath for a maximum of 2 min. The cells were then transferred to a centrifuge tube containing 9 mL DMEM-LG and centrifuged at 1800 rpm for 7 min. Subsequently, the supernatant was discarded, and the washing step was repeated using 6 mL of washing medium to ensure complete removal of DMSO. The pellet was resuspended in complete DMEM-LG containing 10% FBS, 1% sodium pyruvate (Capricorn, NPY.B), and 1% L-glutamine (Capricorn, GLN.B), and then seeded in a 25

cm^2 flask. Later, the cells were incubated at 37ºC in a humidified atmosphere with 5% CO_2.

3.2.3. Seeding and Expansion of UC-MSC

The UC-MSC was purchased (ATCC, PCS-500-010) within the scope of another project (TÜBİTAK Project no. 113S763) and is stored in a liquid nitrogen tank for long-term use. Cells were seeded in DMEM-LG containing 10% FBS, 1% sodium pyruvate, 1% L-glutamine, and 1% pen/strep. When the cells reached 70-80% confluency, cell passaging was performed. The old medium was discarded from the flask, followed by washing with PBS (Phosphate Buffered Saline, Capricorn). Afterwards, adherent cells were detached from the flask using 0.25% Trypsin-EDTA (Gibco, 25200056) solution and kept in an incubator at 37ºC for 2 min. The cells were observed under a microscope (Zeiss, Zen 3.3) to ensure detachment from the flask surface. Deactivation of trypsin was performed after adding 10% FBS-contained DMEM-LG, then the cells were transferred to a centrifuge tube and centrifuged at 1800 rpm for 7 min. Subsequently, the supernatant was discarded, and the pellet was homogenized in complete DMEM-LG. For cell counting, 20 µL of suspended cells were mixed with the same amount of Trypan blue (Sigma, T8154) and added on both sides of a hemocytometer. After performing the calculations, cells were seeded at a density of 10,000 cell/cm^2 in DMEM-LG containing 10% FBS, 1% sodium pyruvate, 1% L-glutamine, and 1% pen/strep, and then incubated at 37ºC in a humidified atmosphere with 5% CO_2. The medium was refreshed twice a week, and the subculturing of UC-MSCs was repeated every 5-6 days.

3.3. Exosome Isolation

To minimize FBS-induced Exo contamination, MSC-qualified FBS was filtered using Amicon® Ultra-Centrifugal Filters (Sigma Aldrich, UFC900324). First, 15 mL of FBS was added to the Amicon® Ultra Filter device and the capped filtered device was placed in a centrifuge rotor. The device was spinned at 3,000xg at 4ºC for 90 min. Finally, the retentate was withdrawn and the ultrafiltrate was stored in centrifuge tubes at -20ºC. For the preparation of Exo-depleted FBS medium, 10% of the ultrafiltrate was

added to DMEM-LG with 1% pen/strep, and the conditioned medium was collected after 48h.

Exo were isolated from UC-MSCs using ultracentrifugation method. The culture media were first centrifuged at 300xg for 10 min to remove dead cells, and the supernatant was centrifuged again at 10,000xg for 30 min to remove cell debris. The supernatant was passed through a 0.22 μm filter then centrifuged in ultracentrifuge tubes at 100,000xg for 70 min. The Exo pellets were resuspended in PBS and centrifuged again at 100,000×g for 70 min at 4°C. Finally, the pellet containing Exo was suspended in 500 μL PBS and stored at -80ºC.

3.4. Preparation of Quercetin-Loaded Exosomes

Que was loaded into Exo using an ultrasonic probe (Bandelin Sonoplus TS103) after Exo isolation. A stock solution was prepared by mixing 4 mL of Exo sample and 1 mg of Que in a glass vial. The following settings were followed with 20% amplitude: 6 cycles of ultrasonication were applied for 3 seconds on /off for 3 min with a 2-minute cooling period in an ice bath between each cycle. After sonication, the prepared Que-Exo were incubated at 37°C for 1h to permit the recovery of the exosomal membrane. They were then stored at -20ºC.

3.5. Characterization of Exosomes and Quercetin-Loaded Exosomes

3.5.1. Western Blot

Exosomal Protein Collection and Concentration Measurement: To identify Exo markers CD9, CD63 and CD81, the pellet collected after ultracentrifugation was suspended with 50 uL 1x RIPA (Radioimmunoprecipitation) lysis buffer (containing 1% protease inhibitor). Exo lysates were boiled at 95°C for 2 min and stored at -20°C.

To determine the Exo protein concentration, the Pierce™ Rapid Gold BCA Protein Assay Kit (Thermo Fisher, A53225) was used. Both the standard and protein samples were prepared according to the kit's protocol, using a dilution ratio of 1:5. The standard protein (BSA) was diluted as shown in **Table 1**. For the protein sample, 2 μL of protein and 8 μL of dH2O were added to reach a final volume of 10 μL. Furthermore, 10 μL was added from both standard and protein samples into a 96-well

plate. The volume of the Working Reagent was calculated as follows: the amount of Reagent A was determined using the formula (#standards + #sample) x (# replication) x (0.2 mL), and the amount of Reagent B was calculated based on its ratio to Reagent A (1:5). In darkness, both reagents were combined in a tube, vortexed, and 200 µL was added to each well containing the standard and protein samples. The absorbance was measured at 480 nm using a microplate reader, and the obtained concentrations were multiplied by 5 to account for the 1:5 dilution ratio.

Table 1: BSA standard's preparation.

Standard	**Diluent volume (µL)**	**BSA volume (µL)**	**Final BSA concentration (µg/mL)**
A	0	150 (stock)	2000
B	31.25	93.75 (stock)	1500
C	50	50 (stock)	1000
D	50	50 (from B)	750
E	50	50 (from C)	500
F	50	50 (from E)	250
G	50	50 (from F)	125
H	80	20 (from G)	25
I	100	0	0

Gel Preparation: The 10% separating gel was poured into the casting module, and isopropanol was added to remove air bubbles and prevent the gel from drying. Once the gel solidified, the isopropanol was poured off and the gel was washed with dH2O until the smell disappeared. Subsequently, the stacking gel was prepared and poured into the casting module, and a 10-well comb was immediately placed. After the gel had completely solidified, it was either used directly or kept at 4°C, wrapped in a wet filter paper, for later use.

Table 2: Preparation of 10% acrylamide gel.

Component	Separating gel	Stacking gel
dH_2O	2.25 mL	2.212 mL
1M Tris HCl	3.75 mL (pH 8.8)	0.38 mL (pH 6.8)
40% acrylamide	2.5 mL	0.225 mL
2% APS	0.5 mL	0.15 mL
1% SDS	1 mL	30 µL
TEMED	10 µL	4 µL
Total	10 mL	3 mL

SDS-PAGE: To load the protein samples, 10 µg of protein, 25% 4X Laemmli Sample Buffer (Bio-Rad, 1610747) (containing 10% 335 mM 2-mercaptoethanol (Neofroxx, 1414ML100)), and RIPA buffer were mixed in a tube to reach a final volume of 20 µL. The gel was placed into a Mini-PROTEAN Tetra Vertical Electrophoresis Cell for Mini Precast Gels (Bio-Rad, 1658004), and 1X Running Buffer (**Table 3**) was added. The 10-well comb was removed, then a syringe was used to wash the wells to ensure they were clean. Both the protein ladder (ThermoFisher Scientific, 26616) and the protein samples were loaded into the wells. Electrophoresis was run at a constant voltage, starting at 100 V for 30 min, and then increasing to 150 V until the protein samples reached near the end of the gel.

Table 3: Preparation of 10X SDS-PAGE Running Buffer.

Component	Amount
Glycine	36 g
Tris	7.575 g
SDS	2.5 g
dH2O	Up to 250 mL

Blotting: The Trans-Blot Turbo RTA Mini PVDF kit (Bio-Rad, 1704272) was used to transfer proteins from the gel to a 0.2 μm PVDF membrane. Two ion reservoir stacks were immersed in 1X Transfer Buffer (**Table 4**) for 2–3 min on a rocking shaker. The PVDF membrane was immersed in 99.9% absolute ethanol for 20–30 seconds until it became translucent, then transferred to 1X Transfer Buffer. The blotting sandwich was assembled at the center of the Blot Turbo Transfer System cassette (Bio-Rad, 1704150). The assembly was arranged in the following order: stack, PVDF membrane, gel, and a final layer of stack. A blot roller was used to remove air bubbles from all layers except the gel. Blotting was performed at a constant current of 1 A, with variable voltage, for 70 min.

Table 4: Preparation of 1X transfer buffer.

Component	Amount	Final concentration
5X transfer buffer	50 mL	1X
EtOH	50 mL	
dH_2O	150 mL	
Total	250 mL	

After blotting, the gel was transferred to Coomassie Blue solution (**Table 5**) and incubated for 45 min, followed by transfer to a Destaining solution (**Table 6**) and overnight incubation on a rocking shaker. The PVDF membrane was transferred to a Blocking solution (**Table 7**) and incubated on a 3D shaker for 1h at room temperature. After blocking, the membrane was not cut, as the targeted proteins were located very close to each other. The membrane was incubated overnight at 4°C in primary antibody solutions (**Table 9**) containing anti-GAPDH (Boster, M00227) at a 1:10,000 dilution, and anti-CD9 (Affinity, AF5139), anti-CD63 (Affinity, AF5117), and anti-CD81 (Affinity, DF2306) primary antibodies, each at a 1:1,000 dilution. The following day, the membrane was incubated for 2h on a 3D shaker at room temperature, followed by three washes with TTBS (**Table 11**), each lasting 5 min. Afterwards, they were

incubated with a secondary antibody solution in darkness for 1h, then the membranes were washed three times with TTBS (each washing lasted for 5 min).

Table 5: Preparation of Coomassie Blue solution.

Component	Amount	Final Concentration
Coomassie Blue	0.5 g	1.1%
MeOH	200 mL	40%
AcOH	5 mL	1%
dH_2O	295 mL	
Total	500 mL	

Table 6: Preparation of Coomassie Destaining solution.

Component	Amount	Final Concentration
MeOH	200 mL	40%
AcOH	5 mL	1%
dH_2O	295 mL	
Total	500 mL	

Table 7: Preparation of Blocking solution.

Component	Amount	Final Concentration
Skim Milk	0.5 g	5%
TWEEN-20	10 µL	0.1%
New TBS	10 mL	

Table 8: Preparation of NEW TBS.

Component	Amount
1M Tris-HCl (pH 7.5)	10 mL
5M NaCl	20 mL
dH2O	960 mL
Total	1000 mL

Table 9: Preparation of Antibody solution.

Component	Amount	Final Concentration
Skim Milk	1.25 g	5%
TWEEN-20	250 µL	1%
New TBS	25 mL	

Table 10: Preparation of 10X TBS.

Component	Amount	Final Concentration
1M Tris-HCl (pH 7.5)	200 mL	200 mM
NaCl	292.2 g	5 M
dH_2O	Up to 1000 mL	

Table 11: Preparation of TTBS.

Component	Amount	Final Concentration
10X TBS	100 mL	1X
TWEEN-20	0.5 mL	0.05%
dH_2O	900 mL	
Total	1000 mL	

WesternBright ECL-HRP substrate (Advansta, ADV-K-12045-C20) was prepared in a 1:1 ratio. The membrane was drained of excess TTBS, and the prepared ECL-HRP substrate was applied to the membrane, followed by a 2-minute incubation. Excess solution was then removed, and the membrane was visualized using the C-Digit Blot Scanner (LI-COR). Band densities were analyzed using the ImageJ program.

3.5.2. Particle Size and Distribution Measurement

The Exo and Que-Exo concentrations and sizes were determined by Dynamic Light Scattering (DLS) method using the Wyatt DynaPro NanoStar device. Both samples were diluted and 2 μL added to a cuvette then placed in the device to record the data. Both the concentrations (particle/mL) and size distributions of Exo and Que-Exo obtained from the medium were determined.

3.5.3. Zeta Potential Analysis

The Anton Paar, Litesizer 500 device was used to determine the stability of Exo and Que-Exo. 700 μL of each samples was added to a folded capillary zeta cell. The result of one repeated measurement was calculated as the mean±standard deviation, and the zeta potential was measured in millivolts (mV).

3.5.4. Transmission Electron Microscopy

Morphological analysis of Exo and Que-Exo was performed using a Thermo Scientific™ Talos L120C Transmission Electron Microscopy (TEM) device. 10 μL of the Exo and Que-Exo samples were each dropped onto a petri dish then was covered with a carbon-coated grid. The samples were kept drying completely at room temperature overnight. Finally, the dried grids were placed on the device via the apparatus, and images were taken at different magnifications.

3.6. Determination of Entrapment Efficiency % for Quercetin-Loaded Exosomes

The Que content in the Exo was determined indirectly by measuring the drug present in the external phase. Unloaded Que was removed by centrifuging the solution at 10,000xg for 10 min at 4°C. The supernatant was transferred to a clean eppendorf

tube, while the pellet (unloaded Que, which is poorly water-soluble) was dissolved in methanol to calculate the loading efficiency of Que. The supernatant containing Que-Exo was then analyzed for drug content using a double beam UV-VIS spectrophotometer at 256 nm and 370 nm. The absorbance values at 256 nm were used in all calculations due to their high consistency. The amount of Que was calculated using a previously constructed calibration curve. The percentage of drug encapsulation in Exo was determined using an indirect method, as shown in the following equation:

$$\text{Encapsulation Efficiency (EE) \%} = \frac{\text{Total amount of drug} - \text{Amount of free drug}}{\text{Total amount of drug}} \times 100$$

3.7. *In Vitro* Release Study of Quercetin-Loaded Exosomes

The *in vitro* release of Que from Que-Exo and Que suspensions were evaluated using the dialysis bag method. A 12–14 kDa pore-size dialysis membrane was pre-soaked in PBS for 1 day before assembling the Franz Cell system to evaluate the release of Que from Exo. The system was kept at 37°C with a stirring speed of 200 rpm. Two Franz Cells were prepared, each containing a receptor compartment filled with 15 mL of warm PBS (pH 7.4) and a magnetic stirring bar. To ensure a total volume of 16 mL in each compartment, an additional 15 mL of PBS was added through the sampling ports. The experiment began by adding 1 mL of Que-Exo to one dialysis bag and 1 mL of Que dissolved in PBS to the other. Samples were collected at predetermined time intervals: 10, 20 min, 1, 6, and 24h. These samples were analyzed using UV-VIS spectrophotometry to generate drug release profiles over time. The data was collected to construct the graph for Que release (%).

3.8. *In Vitro* Cellular Uptake of Quercetin-Loaded Exosomes

To label the Exo and evaluate their uptake by cells, Cytotrace™ CM-DiD (AAT Bioquest, 22060) dye was used. A total of 300 µL of the Exo sample was incubated with 5 µM CM-DiD dye at 37 °C for 30 min. The exosome/dye sample was added to the Amicon® Ultra-Centrifugal Filters, washed with 10 mL of ddH_2O, and then centrifuged at 3,000×g for 30 min at 4°C to remove the unbound dye. HMC3 cells were seeded in a 24-well plate and then treated with the labeled Exo for 3, 6, and 24h. Following treatment, the cells were fixed with 4% PFA, and the nuclei were stained

with DAPI (NEOFROXX, 1322MG005). The samples were then mounted with ProLong™ Glass Antifade Mountant (Thermo Fisher Scientific, P36980) and covered with cover slips. Fluorescence images were taken using a Zeiss fluorescence microscope, and the presence of CM-DiD-labeled Exo within HMC3 cells was examined to confirm Exo uptake.

3.9. Induction of Neuroinflammation Model

To induce activation in HMC3 cells, a sequential stimulation protocol was employed. Once the cells reached approximately 70–80% confluency, they were first treated with 50 µM ATP for 10 min to mimic an acute inflammatory signal and initiate a rapid microglial response. Following this initial stimulation, 1 µg/mL of LPS and 10 ng/mL of IFN-γ were added to the culture medium to further promote a sustained pro-inflammatory activation state. The cells were then incubated under these conditions for 48h, followed by various molecular analyses.

3.10. Experimental Design

The experimental design for this study included eight distinct groups, each structured to evaluate specific aspects of the research objectives. To comprehensively assess cellular and molecular responses, a range of molecular analyses were conducted on all experimental groups. These analyses included pro-inflammatory cytokine analysis using flow cytometer, nitrite measurement to assess nitric oxide production, enzymatic assay to evaluate functional changes in inflammatory, western blotting for protein expression profiling, particularly of signaling molecules such as NF-κB, COX-2, and iNOS to assess their changes under different treatment conditions.

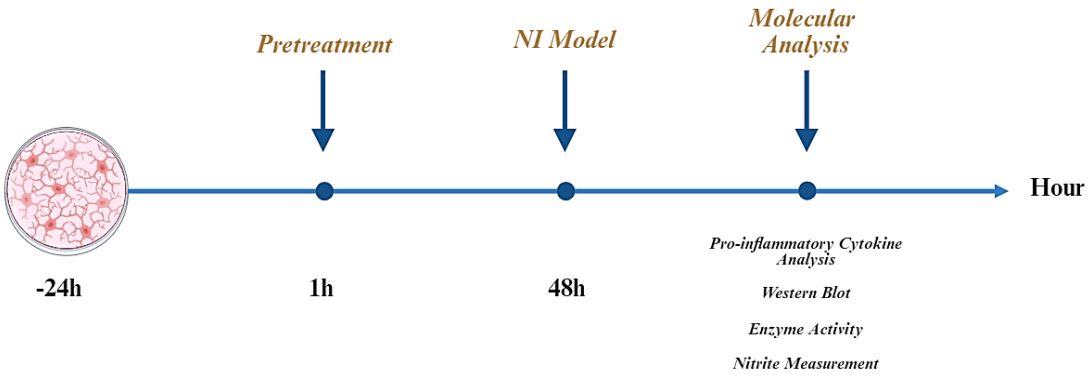

Figure 16: Experiment timeline.

Table 12: Experimental Groups

Groups	Experimental Groups	Description
1	Control (Ctrl)	No application.
2	Exo	Exo application on HMC3
3	Que-Exo	Que-Exo application on HMC3
4	Que	Que application on HMC3
5	NI Model	NI model with LPS and IFN-γ.
6	NI Model + Exo	NI model with LPS and IFN-γ + Exo.
7	NI Model + Que-Exo	NI model with LPS and IFN-γ + Que-Exo.
8	NI Model + Que	NI model with LPS and IFN-γ + Que.

3.11. Molecular analysis

3.11.1. Cell Viability Assay

The cell viability assay was conducted using the MTT method to evaluate the effects of the NI model, Que (MedChemExpress, HY-18095), Exo, and Que-Exo. A total of 10,000 cells were seeded per well in a 96-well plate and treated with various concentrations of the respective agents. Triplicate wells were set up for each experiment. 24h after the treatments, MTT reagent (Roche, 11465007001) was added to the cells, and after 4h, a solubilization buffer was added. The cells were incubated at 37°C with 5% CO_2 for 16h. Finally, absorbance measurements were taken at 570 nm using a spectrophotometer to assess cell viability.

To prepare 100 μM stock solution of quercetin, 10 mg was weighed and dissolved in 330.86 μL DMSO until a homogenized solution was obtained. Subsequently, the solution was divided into 0.2 mL PCR tubes, sealed with aluminum foil, and stored in -20ºC.

The treatment groups were as follows:

NI model: LPS, IFN-γ, LPS + IFN-γ, ATP, ATP + LPS, ATP + IFN-γ, and ATP + LPS + IFN-γ.

Que: 10, 50, 100, 200, 300, 400, and 500 μM.

Exo: 1×10^3, 5×10^3, 1×10^4, 4.94×10^4, 5×10^4, 1×10^5, 5×10^5, 1 x 10^6, and 5 x 10^6.

Que-Exo: 1×10^3, 5×10^3, 1×10^4, 4.94×10^4, 5×10^4, 1×10^5, and 5×10^5.

3.11.2. Cytokine Analysis

Cell culture supernatants were collected 48h after NI induction and stored at −20°C until analysis. The expression levels of the pro-inflammatory cytokine IL-6 secreted by HMC3 microglial cells were quantified using the LEGENDplex™ Human Essential Immune Response Panel (BioLegend, 740929), following the manufacturer's instructions. This bead-based multiplex assay enables the simultaneous detection of multiple cytokines via flow cytometry (Attune™ NxT Acoustic Focusing Cytometer, Thermo Fisher Scientific), offering high sensitivity and specificity.

3.11.3. Nitrite Measurement

Nitrite levels in the cell culture supernatants were quantified using the Griess Reagent (Cell Signaling Technologies, 13547). The standard was prepared by serially diluting the 0.1 M nitrite standard with MEM to obtain the following concentrations: 1.56, 3.13, 6.25, 12.5, 25, 50, and 100 μM. The supernatants were collected from the groups and 50 μL was added each in a 96-well plate, similarly for the nitrite standards. Afterwards, 50 μL Griess Reagent (A mixture of sulfanilamide solution and N-(1-naphthyl)ethylenediamine dihydrochloride (NED) solutions of 1:1 ratio) was added to each well and was incubated for 10 min in darkness. The measurements were obtained at an absorbance of 550 nm.

3.11.4. Enzyme Assay

iNOS enzyme activity measurement: The activity of iNOS was determined using the NOS Activity Assay Kit (Cayman, 781001), following the manufacturer's

instructions. The kit is based on the biochemical principle of converting L-arginine to L-citrulline. The kit measures the rate of citrulline production, thereby providing an indirect assessment of iNOS enzyme activity.

3.11.5. Western Blot

Proteins were isolated from the cells in the experimental groups and their concentrations were determined. 35 μg protein was loaded on 10% SDS-PAGE gel and transferred to PVDF membrane after electrophoresis. The membrane was first blocked with TBS-T containing 5% BSA and then incubated with anti-NFκB (Cell Signaling Technologies, 8242), anti-iNOS (Cell Signaling Technologies, #13120), anti-COX-2 (ThermoFiher Scientific, #35-8200), and anti-GAPDH (Boster, #M00227) antibodies for 1h. After washing, incubation was performed with HRP-conjugated secondary antibody, ECL substrate solution was added, and imaging was performed with C-Digit Blot Scanner. Band intensities were analyzed by ImageJ program.

3.12. Statistical Analysis

All data were expressed as mean ± standard deviation (SD). Statistical analysis was performed using GraphPad Prism software. One-way analysis of variance (ANOVA) was used to compare differences among groups. Statistical significance relative to the control group was indicated by asterisks: *$p<0.05$, **$p<0.01$, ***$p<0.001$, and ****$p<0.0001$. Comparisons with the neuroinflammation group were denoted by number signs: #$p<0.05$, ##$p<0.01$, ###$p<0.001$, and ####$p<0.0001$. Non-significant differences were labeled as “ns.”

4. FINDINGS

4.1. UC-MSC culture conditions

UC-MSCs were subcultured twice a week in a medium containing DMEM-LG containing 15% FBS, and 1% pen/strep. To maintain optimal cell health, they were refreshed every day by removing half of the old and adding half of the new medium. UC-MSCs typically display a fibroblast-like morphology often form colonies (**Figure 17**). Under normal culture conditions, they appear as spindle-shaped or elongated cells. As they proliferate, UC-MSCs maintain a relatively consistent morphology; however, they enlarge and become rounded as the passage number increases. The conditioned media were collected at passage 6.

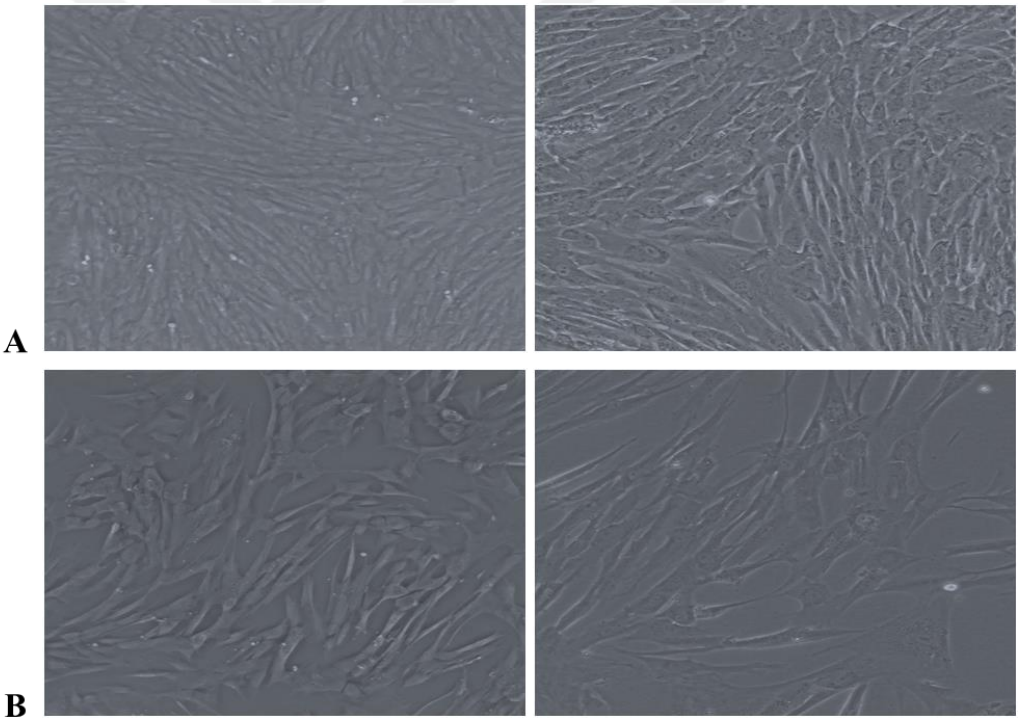

Figure 17: Morphological images of UC-MSC (ATCC PCS-500-010) using 5x and 10x objections of early passages. **A:** Passage 0 and **B:** Passage 4.

Culturing UC-MSCs with Exo-depleted FBS successfully maintained their cellular growth. However, as the cells progressed to later passages, noticeable morphological changes began to emerge. Specifically, the UC-MSCs adopted a wider

and more flattened appearance, deviating from their typical spindle-shaped morphology.

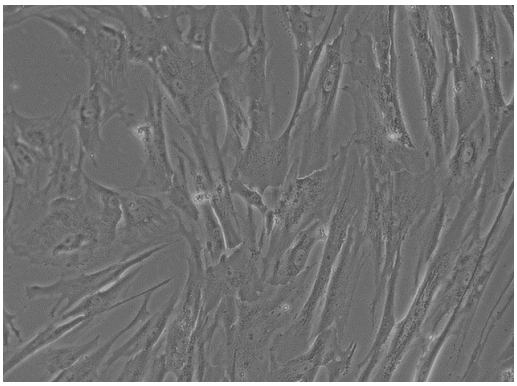

Figure 18: Morphological images of Exo-depleted UC-MSC using 10x objection of passage 6.

4.2. HMC3 culture conditions

HMC3 cells were subcultured twice a week in a medium containing MEM containing 10% FBS, 1% sodium pyruvate, 1% L-glutamine, and 1% pen/strep. Cells were refreshed every day.

HMC3 cells are a heterogeneous population, exhibiting variability in size and shape at the molecular level (**Figure 19**). Over time and with continuous passage particularly between passages 10 and 16, during which molecular analysis was conducted, noticeable changes in cell morphology were observed. Molecular analysis was conducted between passages 10 and 16.

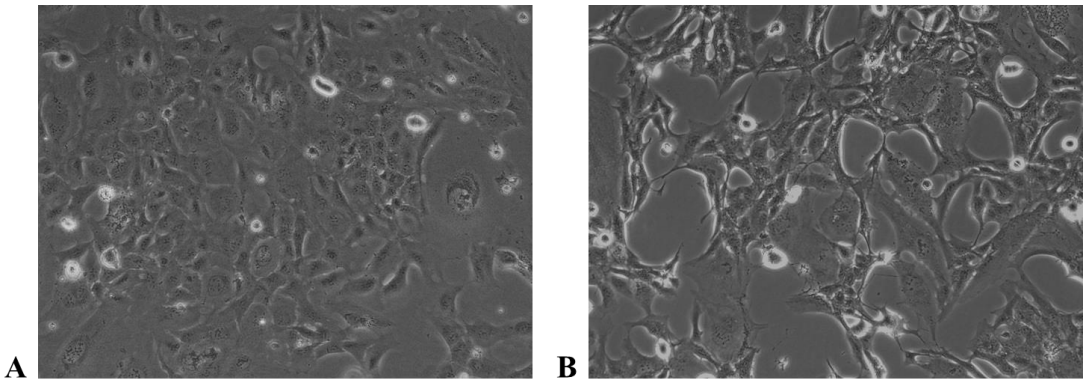

Figure 19: Morphological images of HMC3 (ATCC CRL-3304) using 10x objection; (A) 9th passage, an early passage, and (B) 16th passage, late passage.

4.3. Characterization of exosomes and quercetin-loaded exosomes

Western blot analysis indicated that Exo express specific Exo markers (**Figure 20A**), including CD63, CD81, and CD9. Western blot analysis confirmed the successful isolation and characterization of Exo. Strong bands were observed for CD9, while CD81 and CD63 showed weaker, yet detectable signals.

The zeta potential, which indicates the surface charge and colloidal stability of nanoparticles, was higher for the Que-Exo, with a measurement of -13.9 mV, compared to -3.63 mV for free Exo (**Figure 20B**). The increase in negative charge suggests that loading quercetin improved the stability of the Exo, as a higher zeta potential typically correlates with enhanced stability and reduced likelihood of aggregation.

The size distribution of Exo (**Figure 20C, D**) was altered following Que loading. The DLS indicated that Exo and Que-Exo had mean diameters of 110 nm and 150 nm. The size enlargement suggested that Que loading effectively altered the physical properties of the Exo. In addition, there was a notable difference in the concentration of Exo and Que-Exo, which were both detected by DLS. The concentration of Exo was 4.2×10^7 particles/mL, whereas the Que-Exo's concentration was 4.75×10^6 particles/mL.

TEM images revealed that the Exo and Que-Exo were relatively uniform in size and exhibited a characteristic spherical morphology with well-defined lipid bilayer membranes, consistent with typical exosomal structures (**Figure 20E, F**).

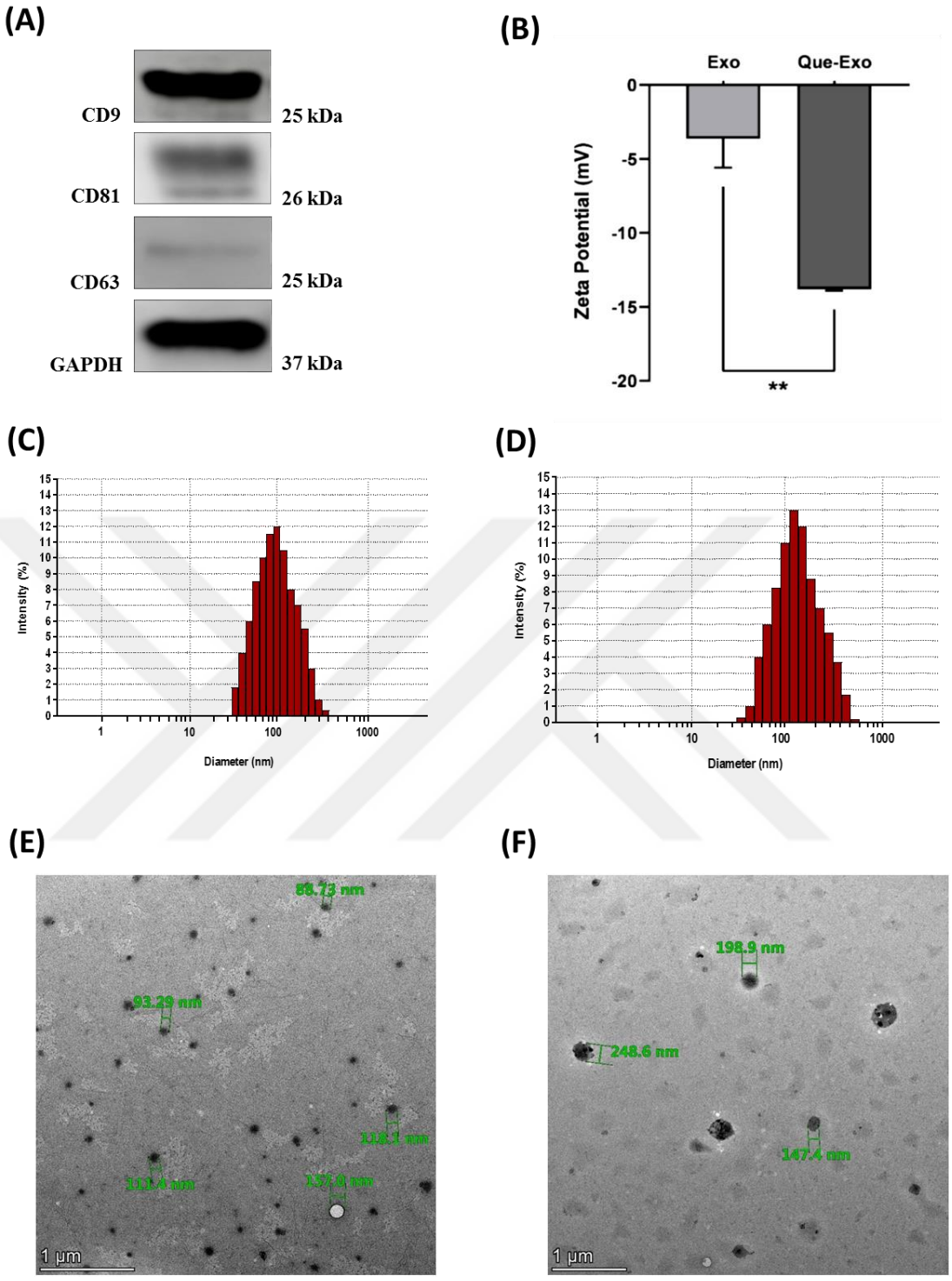

Figure 20: Characterization of Exo and Que-Exo **(A)** Western Blot analysis for Exo markers. (B) Zeta potential analysis of Exo and Que-Exo. Size detection of (C) Exo and (D) Que-Exo using DLS. TEM images of (E) Exo and (F) Que-Exo using 200 nm magnification; scale bar: 1 µm.

4.4. Successful entrapment of quercetin into exosomes

The EE (%) of Que-Exo was quantitatively assessed using the dialysis bag method. The EE was calculated to be 46.26%, indicating that nearly half of the initially added Que was successfully entrapped within the Exo. Hence, this suggests effective loading of the hydrophobic compound into the exosomal structure, likely due to hydrophobic interactions between Que and the lipid bilayer of the Exo.

The amount of Que was calculated using the constructed calibration curve at 256 nm absorbance (**Figure 21**).

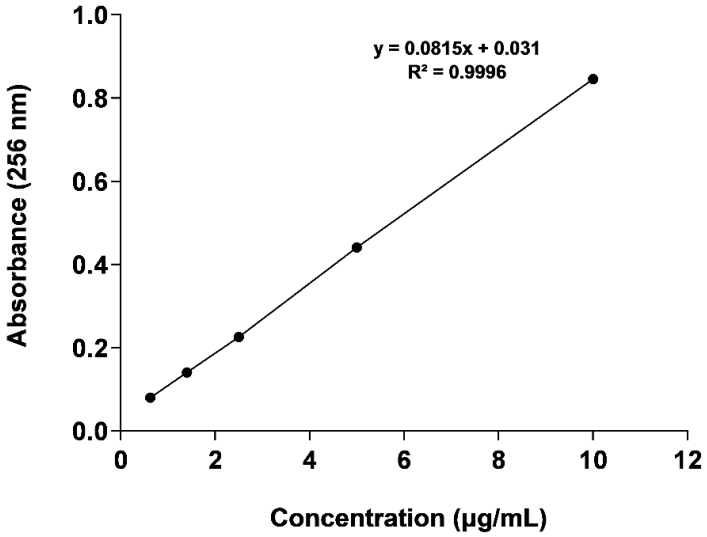

Figure 21: UV-Spectrophotometry method. Calibration curve of Que with 256 nm absorbance.

4.5. Successful drug release

The release of the Que-Exo formulation (**Figure 22**) was significantly higher than that of Que at all measured time points. The release of Que-Exo began after 30 min, while that of free Que started after 10 min. Moreover, both completed their release by 6h. Que-Exo exhibited a rapid and sustained release profile, reaching slightly above 100% by 6h and maintaining this level up to 24h. In contrast, Que showed a lower release, peaking at approximately 42.17% at 6h and slightly declining by 24h. These results suggested that exosomal encapsulation enhanced the solubility and release of Que, potentially improving its bioavailability and therapeutic effectiveness.

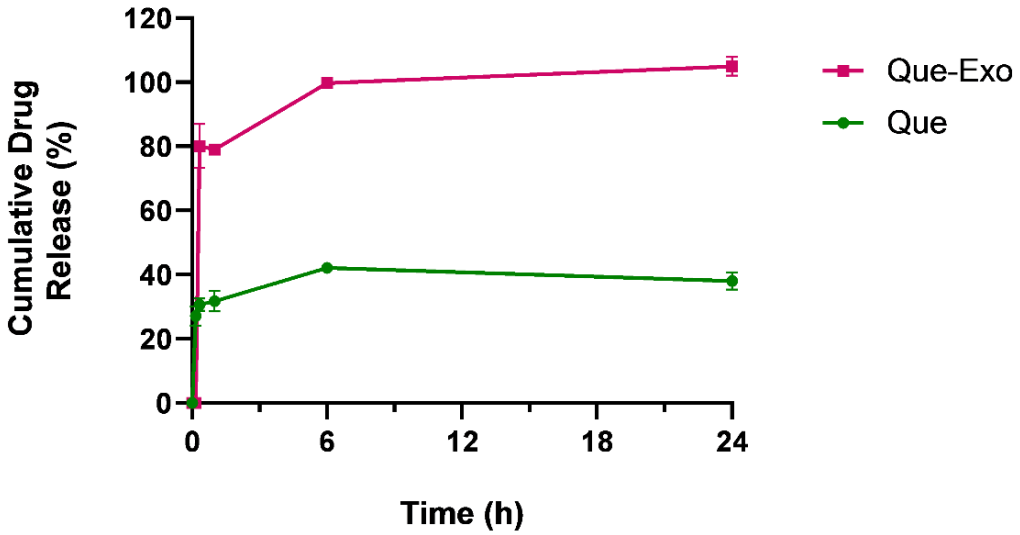

Figure 22: The drug release study of Que-Exo and Que over a 24-hour period.

4.6. Successful quercetin-loaded exosomes uptake by HMC3 cells

To investigate the time-dependent uptake of Exo by HMC3 cells, they were incubated with CM-DiD-labeled Exo and monitored at different time points using fluorescence microscopy (**Figure 23**). The CM-DiD dye selectively labeled the lipid membrane of the Exo, while DAPI staining was used to visualize the cell nuclei.

At the 3-hour time point, no CM-DiD fluorescence signal was observed around the cells, indicating a lack of Exo internalization at this early stage. After 6h of incubation, weak CM-DiD fluorescence began to appear around the nucleus region of the cells, suggesting the onset of Exo uptake. By 24h, a notable increase in CM-DiD signal intensity was observed, with widespread accumulation of labeled Exo around the nucleus of the HMC3 cells. These results indicate that Exo uptake by microglial cells occurs gradually over time, becoming markedly more pronounced by 24h of incubation.

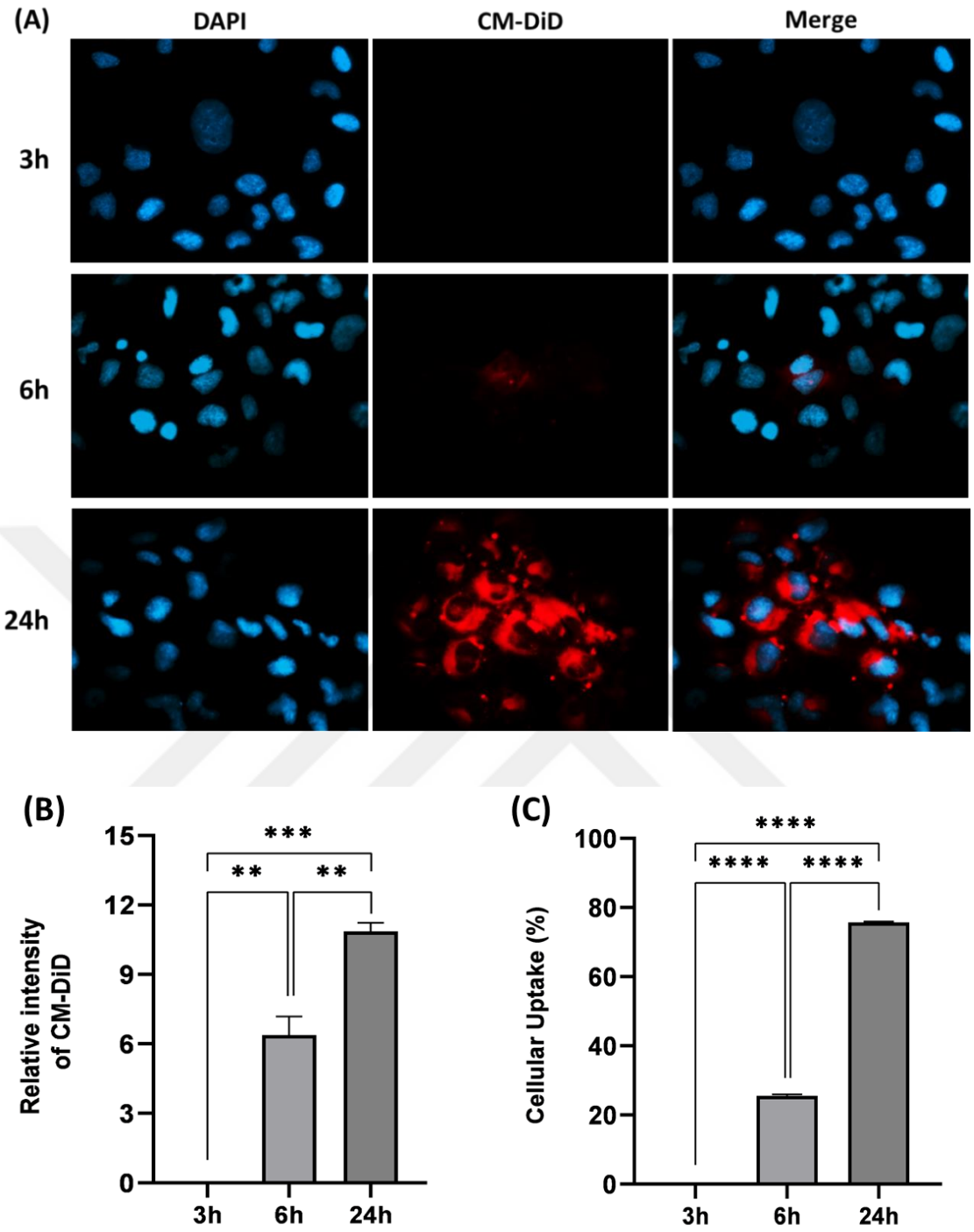

Figure 23: Cellular uptake of CM-DiD labeled Exo with their accumulation around the nucleus. Red fluorescence signals show Exo while blue refers to the stained nuclei with DAPI. (A) Fluorescent images of HMC3 cells obtained after 3, 6, and 24h using 40x magnification; scale bar: 20 μm. (B) CM-DiD-labeled Exo's intensity. (C) Percentage of HMC3 cells that had internalized the CM-DiD dye.

4.7. Assessment of HMC3 cell viability upon different treatments

To evaluate the effects of several compounds on the viability of microglial cells, a comprehensive cell viability analysis was conducted using HMC3 cell line. The goal was to assess how inflammatory stimuli and potential therapeutic agents, such as Exo, Que-Exo, and Que, influence cell viability under both normal and NI conditions**.**

As a preliminary step, different agents commonly used to induce NI were tested for their impact on HMC3 viability. Treatment with ATP significantly reduced cell viability to 64%, indicating high cytotoxicity. LPS caused a milder reduction, lowering viability to 88%, whereas IFN-γ unexpectedly increased viability to 104%, suggesting a possible stimulatory effect on cell proliferation or survival mechanisms in this context (**Figure 24**).

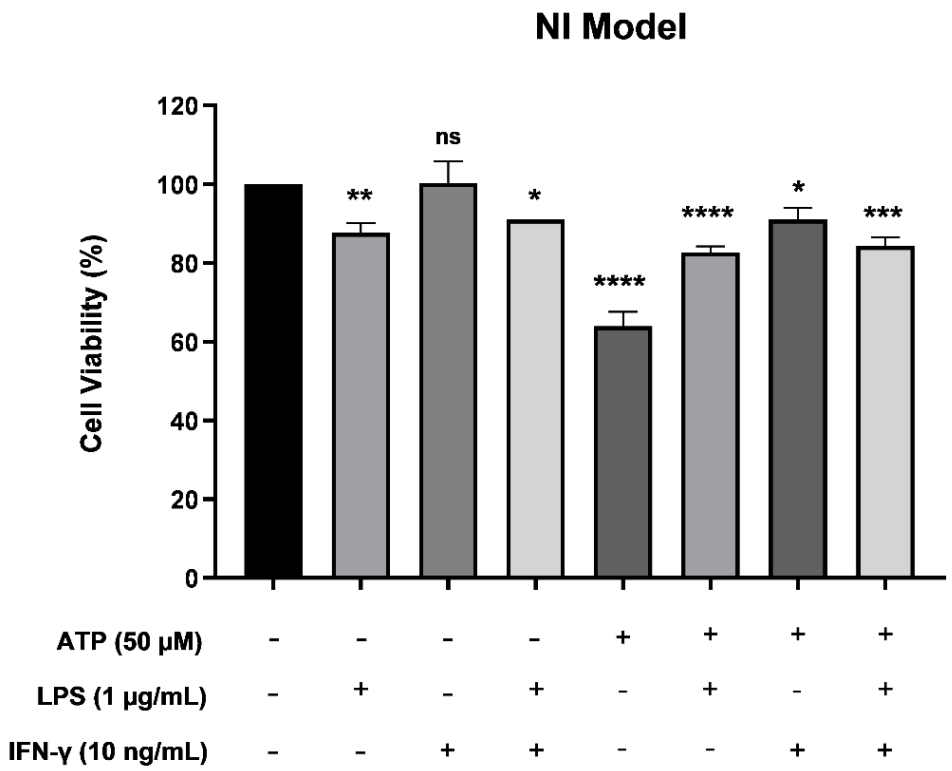

Figure 24: Measurement of HMC3 cell viability after treatment with ATP, LPS, and IFN-γ; n=2; mean ± SD.

Cell Viability Assay of Que (**Figure 25**): At a lower concentration of 10 µM, Que significantly enhanced cell viability, reaching 112%, indicating a beneficial or

protective effect on the cells at this dose. However, as the concentration of Que increased, its effect on cell viability became detrimental. At 50 µM, cell viability dropped to 94%, and further increasing the concentration to 500 µM caused a dramatic decline in cell viability to 44%. This sharp decrease suggested that higher concentrations of Que were toxic to HMC3 cells.

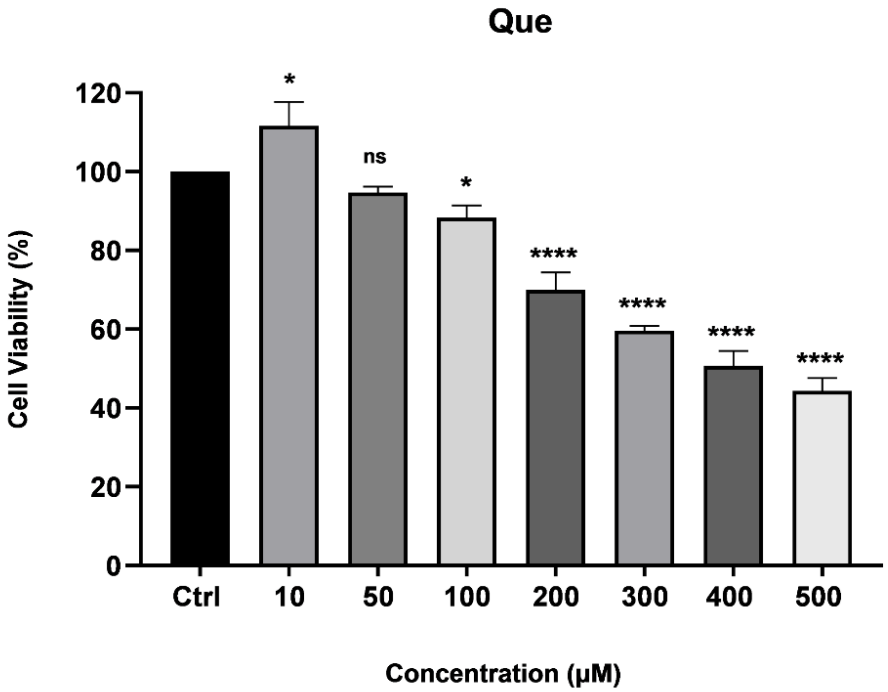

Figure 25: Measurement of HMC3 cell viability after Que treatment with different concentrations (µM); n=2; mean ± SD.

Cell Viability Assay of Exo (**Figure 26**) and Que-Exo (**Figure 27**): The tested concentrations of Exo and Que-Exo ranged from 1×10^3 to 5×10^5 particle/mL. For Exo, concentrations between 1×10^3 and 1×10^5 particle/mL had no considerable effect on HMC3 cell viability. However, from 5×10^4 and 5×10^6 particle/mL, a gradual decline in cell viability was detected. Similarly, for Que-Exo, concentrations between 1×10^3 and 1×10^5 particles/mL did not affect cell viability. Nevertheless, starting from 4.94×10^4 to 5×10^5 particles/mL, a gradual decline in cell viability was observed, indicating a potential dose-dependent effect of Que-Exo.

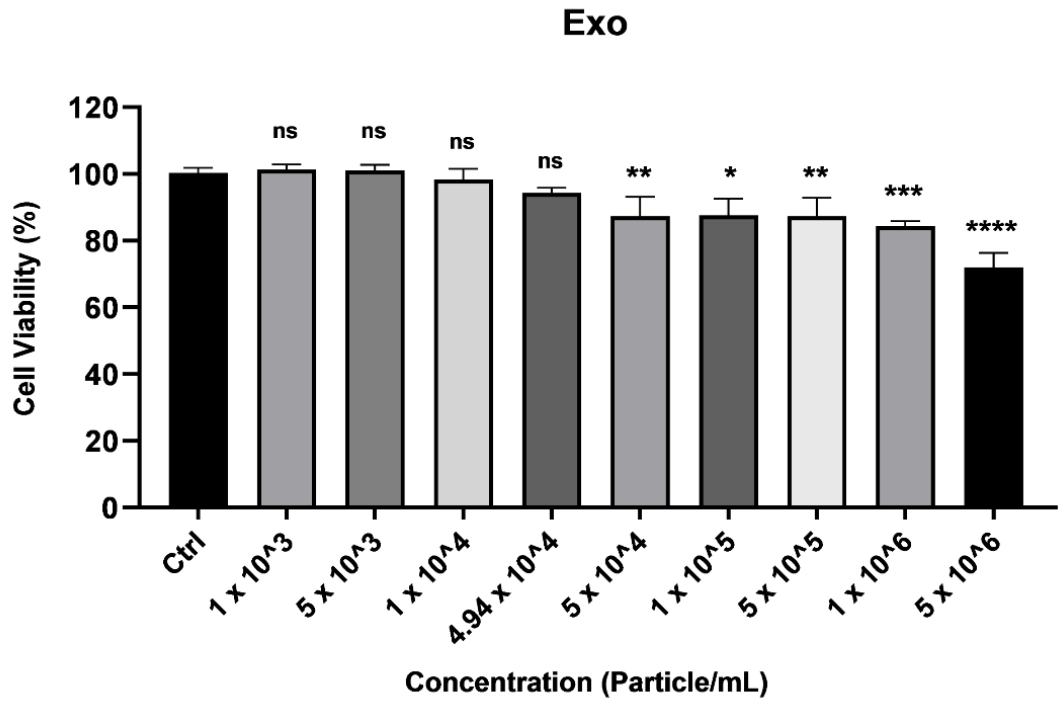

Figure 26: Measurement of HMC3 cell viability after Exo treatment with different concentrations (particle/mL); n=3; mean ± SD.

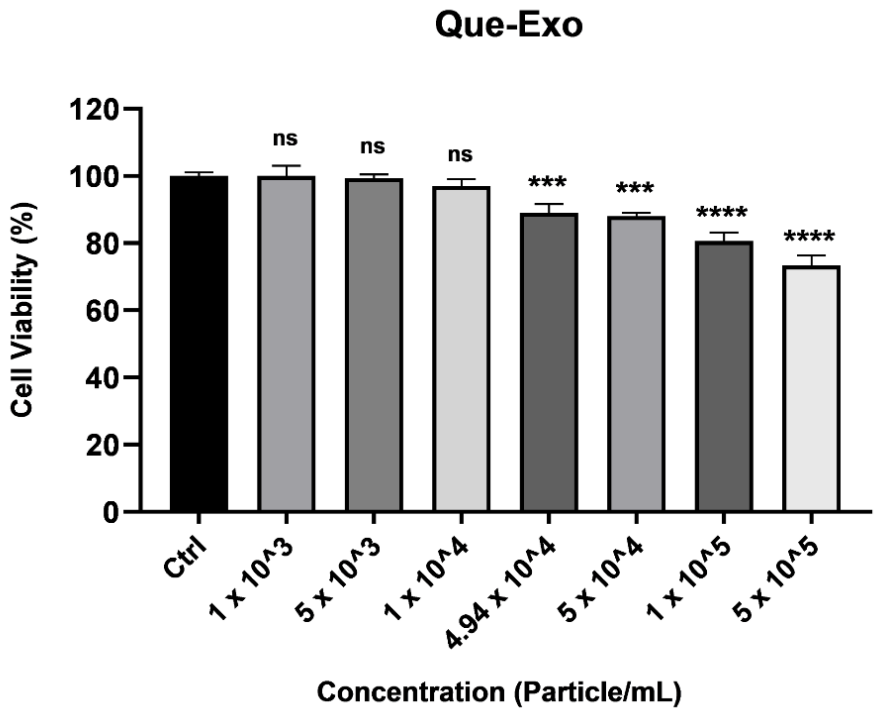

Figure 27: Measurement of HMC3 cell viability after Que-Exo treatment with different concentrations (particle/mL); n=3; mean ± SD.

Under normal conditions (**Figure 28**), 1h treatment with Exo, Que-Exo, and Que each led to a slight but statistically significant decrease in cell viability relative to the untreated control group. Cells treated with Exo and Que-Exo showed comparatively milder reductions in viability, while no toxicity was observed when treated with Que. However, under NI conditions, a marked shift was observed. All three treatments—Exo, Que-Exo, and Que—led to a significant increase in cell viability compared to the NI group. Among the treatments, Que-Exo demonstrated the most pronounced restorative effect, surpassing both Exo and Que alone. These findings highlight that while the treatments might mildly suppress viability under normal conditions, they confer strong protective and potentially therapeutic benefits in the context of neuroinflammation—particularly when Que is delivered via Exo.

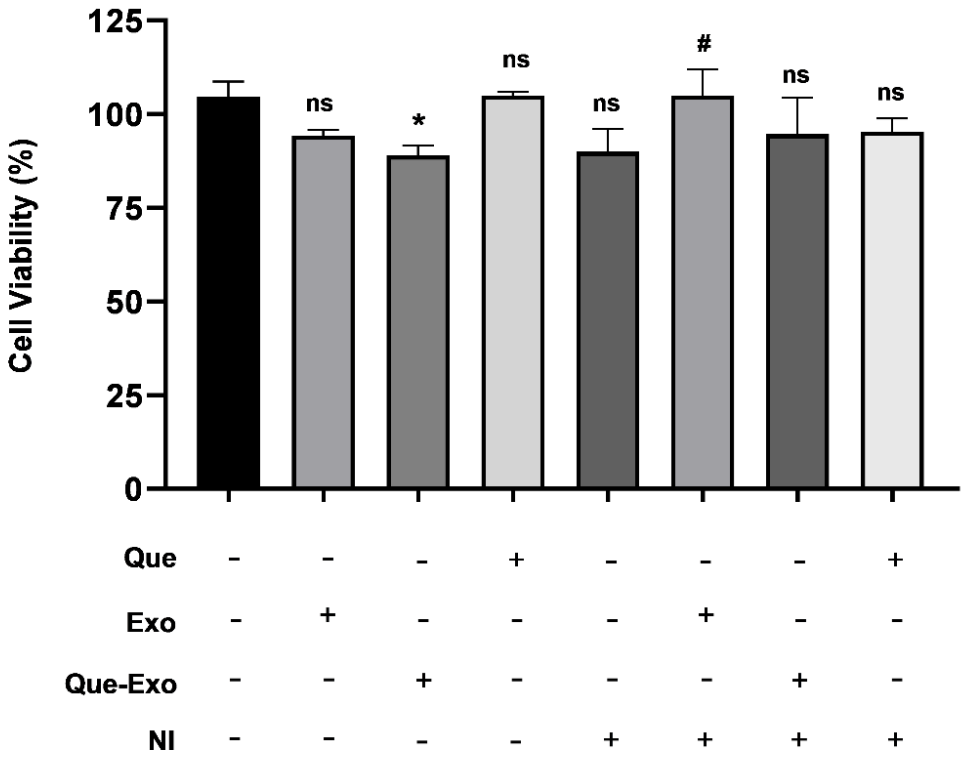

Figure 28: Measurement of HMC3 viability under 1h pretreatment with Exo, Que-Exo, and Que under normal and NI conditions; n=2; mean ± SD.

4.8. Quercetin-loaded exosomes attenuate IL-6 expression in neuroinflammation

The expression level of the pro-inflammatory cytokine IL-6 (**Figure 29**) was markedly elevated in the NI group following stimulation with LPS and IFN-γ. This represents a significant increase relative to the unstimulated control group, demonstrating the successful generation of an inflammatory response.

In contrast, pretreatment with either Exo or Que led to a modest reduction in IL-6 levels, where they exerted a partial anti-inflammatory effect relative to the NI group. Notably, in the Que-Exo-pretreated group, IL-6 expression decreased significantly. This substantial reduction highlights the enhanced therapeutic and synergistic efficacy of the combined formulation, suggesting that the exosomal delivery of quercetin may improve its bioavailability and anti-inflammatory activity.

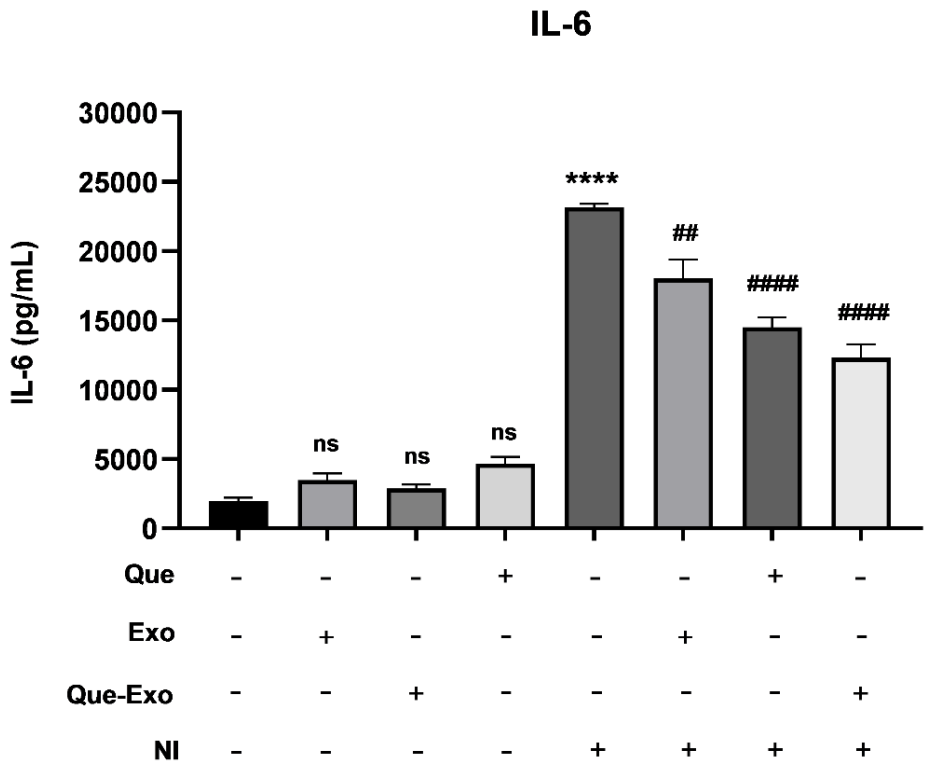

Figure 29: Measurement of IL-6 pro-inflammatory cytokine among the experimental group; n=2; mean ± SD.

4.9. Quercetin-loaded exosomes inhibit the NF-κB pathway activated by LPS

According to the Western blot results (**Figure 30**), the NI group demonstrated a decline in cytoplasmic NF-κB expression relative to the control, which is contrary to the expected increase typically associated with inflammatory activation. This suggests successful translocation of NF-κB from the cytoplasm to the nucleus. However, Exo, Que, and Que-Exo pretreatments led to an increase in cytoplasmic NF-κB expression, indicating their potential to suppress NF-κB nuclear translocation. These treatments, especially Que-Exo, kept NF-κB in the cytoplasm, leading to higher cytoplasmic expression levels.

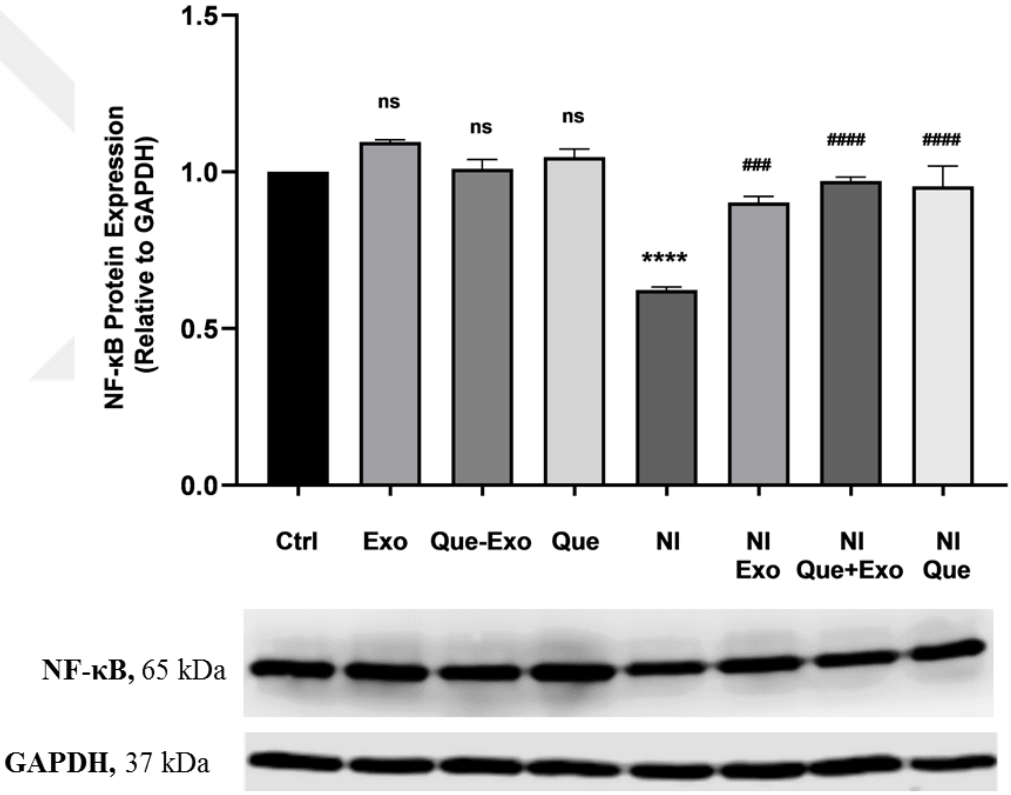

Figure 30: Protein expression levels of NF-κB; n=3; mean ± SD.

4.10. Quercetin-loaded exosomes inhibit pro-inflammatory enzymes in HMC3 cells

The anti-inflammatory potential of Que-Exo was evaluated by measuring nitrite production and iNOS protein expressions and enzyme activities, which are key indicators of inflammatory responses in microglia.

iNOS enzyme activity was assessed under various treatment conditions to evaluate the anti-inflammatory potential of Que-Exo (**Figure 31**). In the NI group, a considerable escalation in iNOS activity was detected, confirming the successful induction of an inflammatory state. In contrast, the NI+Exo and NI+Que groups exhibited only modest reductions in iNOS activity, indicating minimal anti-inflammatory effects.

Notably, pretreatment with Que-Exo showed a marked suppression of iNOS activity compared to Exo and Que treatments alone, demonstrating an enhanced inhibitory effect.

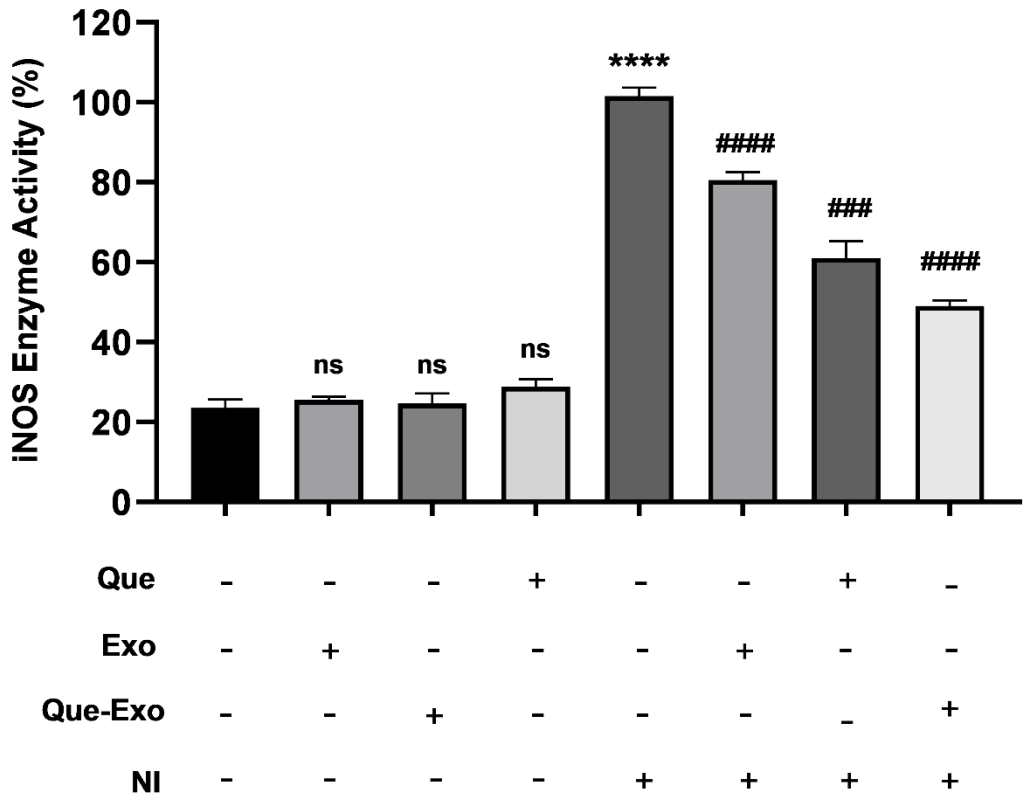

Figure 31: Measurement of iNOS enzyme activity; n=2; mean ± SD.

Nitrite levels were quantified using the Griess reagent kit to indirectly assess NO production, as it is a primary reactive species synthesized by iNOS during inflammatory responses. Nitrite levels (**Figure 32**) were elevated in the NI group, confirming successful induction of inflammation. Treatments with Exo, Que-Exo, and Que alone did not increase nitrite levels relative to the control group. Importantly, pre-treatment of Exo and Que with NI model slightly reduced nitrite concentration compared to NI group. Pre-treatment of Que-Exo demonstrated a marked anti-inflammatory effect, where it decreased nitrite levels compared to NI group.

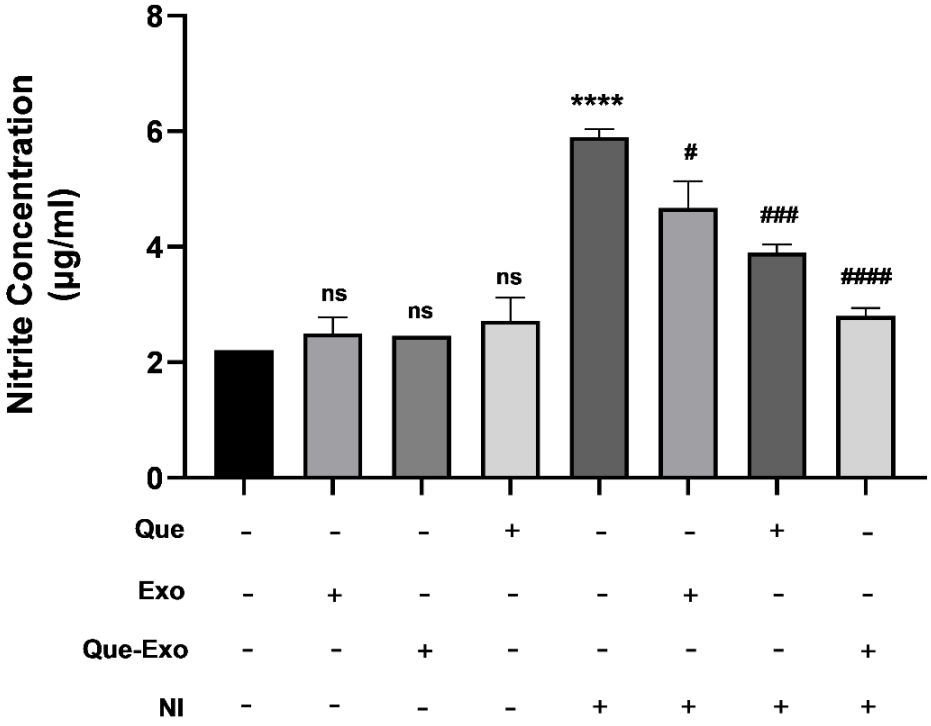

Figure 32: Measurement of nitrite concentrations secreted by HMC3 cells among the groups; n=3; mean ± SD.

The protein expression levels of iNOS and COX-2 were further investigated using Western blot to evaluate their regulation under different treatment conditions. In the analysis of iNOS protein expression (**Figure 33**), a slight increase was observed in the NI group relative to the control, representing an elevation in the inflammatory response following the induction of the neuroinflammatory condition. NI+Exo and NI+Que groups led to a slight reduction in iNOS levels, suggesting a mild anti-inflammatory effect exerted by both agents individually. Notably, pretreatment with

Que-Exo demonstrated a significant decrease in iNOS expression compared to the NI group.

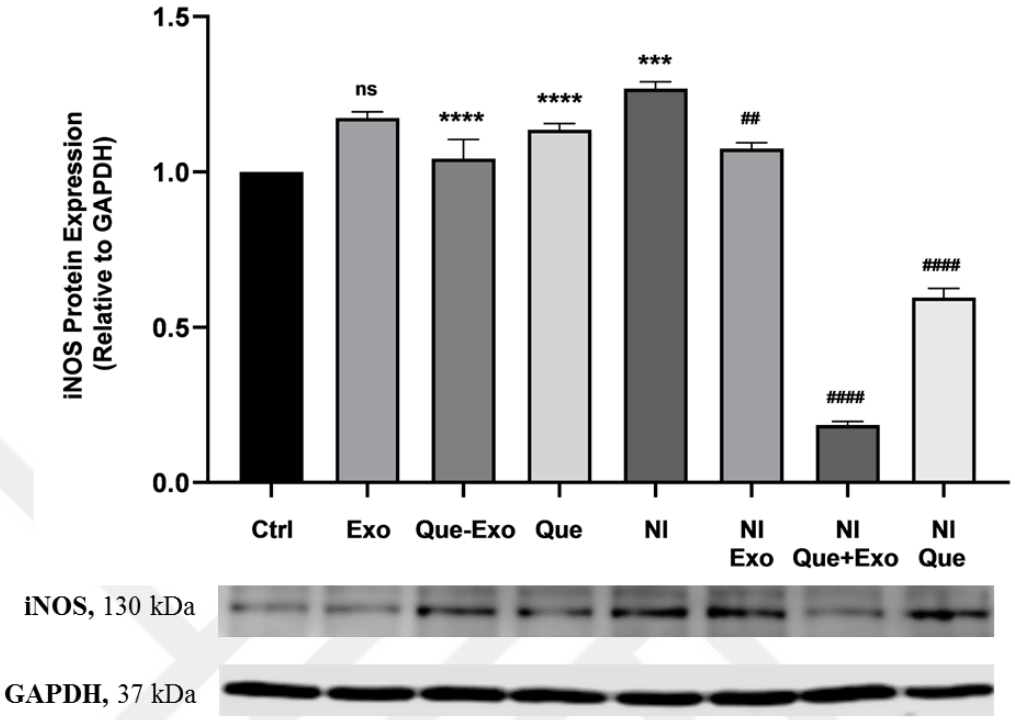

Figure 33: Protein expression levels of iNOS; n=3; mean ± SD.

For COX-2 expression (**Figure 34**), a slight increase was detected in the NI group relative to the control. Pretreatment with Exo and Que resulted in a mild decrease in COX-2 levels. Moreover, the group pretreated with Que-Exo also demonstrated a considerable decrease in COX-2 expression compared to the NI group. Although the reduction was not as pronounced as observed for iNOS in the same group, it still suggests that Que-Exo can attenuate inflammatory signaling, due to synergistic or enhanced anti-inflammatory effect resulting from the combination of Que and Exo-based delivery, highlighting the potential therapeutic advantage of Que-Exo in mitigating neuroinflammation.

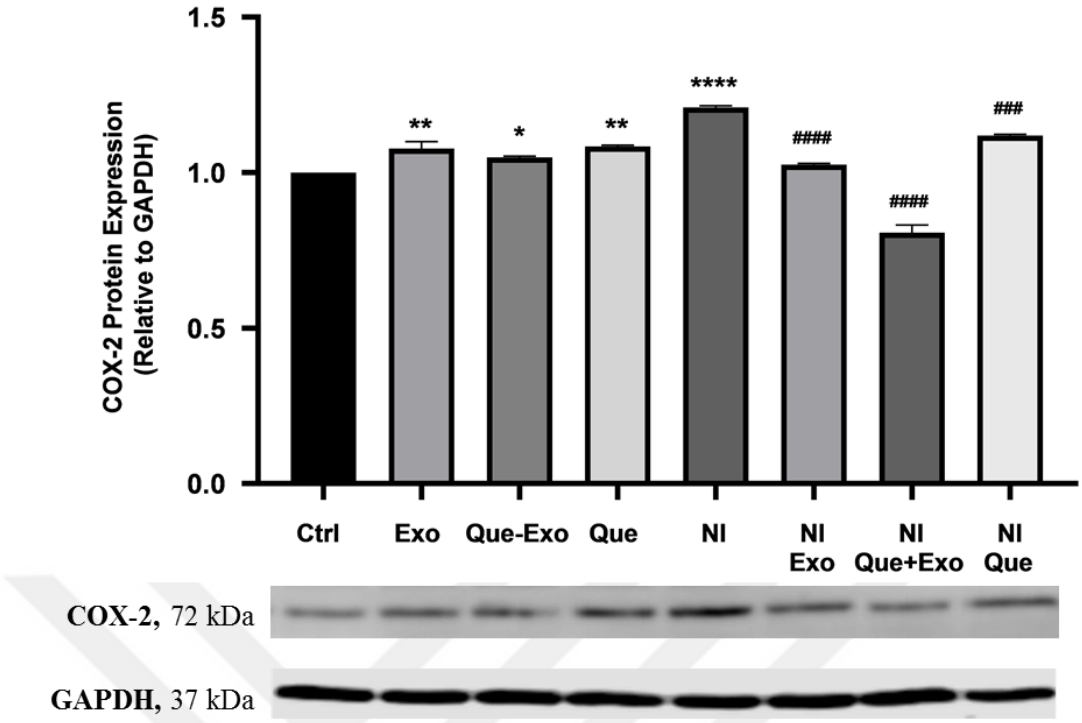

Figure 34: Protein expression levels of COX-2; n=3; mean ± SD.

5. DISCUSSION

NDs, including AD, PD, and HD, are fatal disorders marked by the progressive and persistent deterioration of brain function and structure. Neuroinflammation, mediated by microglia, is a central contributor to disease progression. Microglia, the intrinsic immune cells of the CNS, act as primary responders to injury and infection. Nonetheless, their persistent activation results in the secretion of neurotoxic agents, including as pro-inflammatory cytokines, enzymes, nitric oxide, and reactive oxygen species, which ultimately facilitate neuronal injury and cell demise. Therefore, modulating microglial activation constitutes an essential therapeutic target in the treatment of NDs.

Quercetin, a naturally occurring flavonoid present in various fruits and vegetables, has shown considerable potential in mitigating neuroinflammation owing to its powerful antioxidant and anti-inflammatory characteristics. It inhibits Microglial and astrocyte activation, reduces the expression of pro-inflammatory cytokines such as TNF-α and IL-6, and modulates signaling pathways like NF-κB and MAPK that are central to neuroinflammatory responses. These properties make quercetin a promising treatment for NDs characterized by persistent inflammation. However, despite its promising bioactivity, the application of quercetin is limited by its poor water solubility, low bioavailability, and swift metabolism, which restricts its ability to reach effective concentrations in the CNS. These limitations have driven research into novel delivery systems, such as nanoparticle or exosome-based carriers, to enhance its therapeutic efficacy in targeting neuroinflammation.

In this study, we explored the therapeutic potential of exosome-based delivery of quercetin, in an *in vitro* model of neuroinflammation using HMC3 cell line. The neuroinflammation model had been previously optimized in our lab, where the most suitable combination of substances for inducing inflammation was determined to be 50 μM ATP, followed by 1 μg/ml LPS and 10 ng/ml IFN-γ. This model was then used to assess the effects of quercetin-loaded exosomes on inflammation as part of the hypothesis.

Que-Exo effectively increased the cytoplasmic expression of NF-κB by preventing its translocation to the nucleus, a critical step required for the activation of pro-inflammatory gene expression. By inhibiting this translocation, Que-Exo disrupted the NF-κB signaling cascade and consequently suppressed the transcription of various pro-inflammatory mediators.

In this study, IL-6 expression was markedly elevated in the neuroinflammation group following stimulation with LPS and IFN-γ, confirming the successful activation of an inflammatory response in HMC3 cells. This highlights that the pro-inflammatory cytokine IL-6 is involved in the progression of neuroinflammatory responses. Pretreatment with either Exo or Que led to a slight reduction in IL-6 levels, indicating that both agents possess some inherent anti-inflammatory properties. However, their individual effects appeared limited in suppressing the strong cytokine response triggered by the inflammatory stimuli. Nevertheless, the combination of exosomes and quercetin resulted in a pronounced suppression of IL-6 expression. This outcome strongly suggests a **"synergistic effect"** between the bioactive compound and its exosomal carrier. The use of exosome as a delivery vehicle likely enhanced the cellular uptake and stability of quercetin, improving its ability to modulate inflammatory signaling pathways inclusing NF-κB, which regulates IL-6 production.

Our findings revealed that Que-Exo induced a considerable decline in iNOS and COX-2 expressions, supporting the hypothesis that these two pro-inflammatory enzymes are transcriptionally regulated by NF-κB. Their downregulation further confirms the effective inhibition of the NF-κB signaling pathway. These differences may reflect the sensitivity of iNOS and COX-2 expression to quercetin concentration and intracellular availability, with iNOS potentially being more responsive to antioxidant and anti-inflammatory modulation.

NO is a key mediator of neuroinflammatory damage and is primarily produced by iNOS in activated microglia. Under pathological conditions, excessive NO contributes to oxidative stress and neuronal injury. In our study, iNOS expression was found to be slightly elevated in the neuroinflammation group compared to the control,

which was consistent with the increased NO production measured via the Griess Reagent assay. Pretreatment with Exo or Que led to a slight decrease in both iNOS expression and nitrite levels, suggesting some suppression of the inflammatory response. Notably, the group pretreated with Que-Exo exhibited a significant reduction in iNOS expression and a corresponding decrease in nitrite concentration, as determined by the Griess Reagent assay. This parallel decline in both iNOS and NO levels reinforces the anti-inflammatory efficacy of Que-Exo and indicates that the inhibition of iNOS-mediated NO production is a key mechanism by which Que-Exo mitigates neuroinflammation.

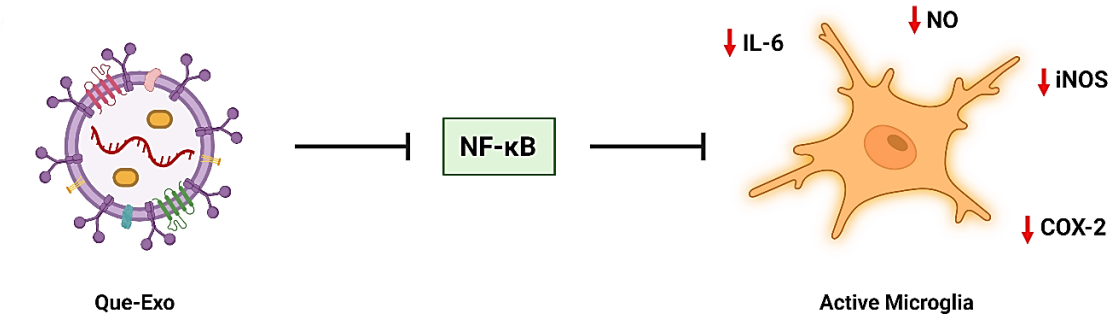

Figure 35: The schematic illustration outlines the fundamental process by which Que-Exo exert their anti-inflammatory effects.

The observed biological outcomes underscore the therapeutic potential of exosome-mediated drug delivery, but also point to several challenges that must be addressed. Most importantly, the mechanism of cellular uptake, intracellular trafficking, and drug release from exosomes remains incompletely understood and warrants further investigation. Moreover, the moderate drug loading efficiency observed with sonication suggests that alternative loading methods, such as electroporation, extrusion, or chemical conjugation, should be explored to enhance drug incorporation without compromising exosome integrity.

In brief, this study provides compelling evidence that Que-Exo represent a promising nanotherapeutic platform for the modulation of microglia-mediated neuroinflammation. Through a combination of physicochemical characterization and biological assessment, we demonstrated their capability to deliver bioactive compounds

with improved stability and cellular response. With further optimization and *in vivo* validation, this strategy has great potential for developing targeted therapies for NDs.

6. CONCLUSION & RECOMMENDATIONS

In this study, the therapeutic potential of Que-loaded Exo was investigated in the context of microglia-mediated neuroinflammation. An *in vitro* model of neuroinflammation was established using HMC3 cell line, and modulatory effect of quercetin, when delivered via exosomes, was assessed by evaluating COX-2 and iNOS activities, nitrite measurement, and NF-κB, iNOS, COX-2 protein expressions, which are critical indicators of inflammatory response.

It was concluded that Que-Exo exhibited a more pronounced anti-inflammatory effect compared to Exo and Que, suggesting that Exo delivery enhances the bioavailability and cellular uptake of Que. Furthermore, Que-Exo demonstrated a sustained modulatory effect, supporting their potential in targeting microglial activation and preventing neurodegenerative progression.

Although Exo are widely regarded as potentia nanocarriers for drug delivery owing to their biocompatibility and ability to bypass biological barriers, our experimental results revealed that high concentrations of Exo exhibited cytotoxic effects. In particular, increasing the dose of Exo led to a marked reduction in cell viability, indicating a dose-dependent toxicity. This unexpected outcome highlights a critical limitation in the application of Exo, especially when high doses are required to achieve therapeutic efficacy. The observed cytotoxicity may be attributed to the accumulation of Exo in the cellular environment, potential immune responses, or interference with cellular signaling pathways. These findings emphasize the need for developing alternative strategies that can maintain effective drug delivery without compromising cell health.

RESOURCES

Abbaszadeh, H., Ghorbani, F., Derakhshani, M., Movassaghpour, A. A., Yousefi, M., Talebi, M., & Shamsasenjan, K. (2020). Regenerative potential of Wharton's jelly-derived mesenchymal stem cells: A new horizon of stem cell therapy. In Journal of Cellular Physiology (Vol. 235, Issue 12, pp. 9230–9240). Wiley-Liss Inc. https://doi.org/10.1002/jcp.29810

Anand, S., Samuel, M., Kumar, S., & Mathivanan, S. (2019). Ticket to a bubble ride: Cargo sorting into exosomes and extracellular vesicles. Biochimica et Biophysica Acta (BBA) - Proteins and Proteomics, 1867(12), 140203. https://doi.org/10.1016/j.bbapap.2019.02.005

Ashour, A. A., El-Kamel, A. H., Mehanna, R. A., Mourad, G., & Heikal, L. A. (2022). Luteolin-loaded exosomes derived from bone marrow mesenchymal stem cells: a promising therapy for liver fibrosis. Drug Delivery, 29(1), 3270–3280. https://doi.org/10.1080/10717544.2022.2142700

Barczuk, J., Siwecka, N., Lusa, W., Rozpędek-Kamińska, W., Kucharska, E., & Majsterek, I. (2022). Targeting NLRP3-Mediated Neuroinflammation in Alzheimer's Disease Treatment. In International Journal of Molecular Sciences (Vol. 23, Issue 16). MDPI. https://doi.org/10.3390/ijms23168979

Barrès, C., Blanc, L., Bette-Bobillo, P., André, S., Mamoun, R., Gabius, H.-J., & Vidal, M. (2010). Galectin-5 is bound onto the surface of rat reticulocyte exosomes and modulates vesicle uptake by macrophages. Blood, 115(3), 696–705. https://doi.org/10.1182/blood-2009-07-231449

Benameur, T., Soleti, R., & Porro, C. (2021). The potential neuroprotective role of free and encapsulated quercetin mediated by mirna against neurological diseases. In Nutrients (Vol. 13, Issue 4). MDPI AG. https://doi.org/10.3390/nu13041318

Benmerah, A., Bayrou, M., Cerf-Bensussan, N., & Dautry-Varsat, A. (1999). Inhibition of clathrin-coated pit assembly by an Eps15 mutant. Journal of Cell Science, 112(9), 1303–1311. https://doi.org/10.1242/jcs.112.9.1303

Carsillo, M., Kutala, V. K., Puschel, K., Blanco, J., Kuppusamy, P., & Niewiesk, S. (2009). Nitric oxide production and nitric oxide synthase type 2 expression by cotton rat (Sigmodon hispidus) macrophages reflect the same pattern as human macrophages. Developmental and Comparative Immunology, 33(5), 718–724. https://doi.org/10.1016/j.dci.2008.12.004

Che, J., Wang, H., Dong, J., Wu, Y., Zhang, H., Fu, L., & Zhang, J. (2024). Human umbilical cord mesenchymal stem cell-derived exosomes attenuate neuroinflammation and oxidative stress through the NRF2/NF-κB/NLRP3 pathway. CNS Neuroscience and Therapeutics, 30(3). https://doi.org/10.1111/cns.14454

Chen, Y., Ye, X., Escames, G., Lei, W., Zhang, X., Li, M., Jing, T., Yao, Y., Qiu, Z., Wang, Z., Acuña-Castroviejo, D., & Yang, Y. (2023). The NLRP3 inflammasome: contributions to inflammation-related diseases. In Cellular and Molecular Biology Letters (Vol. 28, Issue 1). BioMed Central Ltd. https://doi.org/10.1186/s11658-023-00462-9

Chiang, M. C., Tsai, T. Y., & Wang, C. J. (2023). The Potential Benefits of Quercetin for Brain Health: A Review of Anti-Inflammatory and Neuroprotective Mechanisms. In International Journal of Molecular Sciences (Vol. 24, Issue 7). Multidisciplinary Digital Publishing Institute (MDPI). https://doi.org/10.3390/ijms24076328

Colombo, M., Raposo, G., & Théry, C. (2014). Biogenesis, Secretion, and Intercellular Interactions of

Exosomes and Other Extracellular Vesicles. Annual Review of Cell and Developmental Biology, 30(1), 255–289. https://doi.org/10.1146/annurev-cellbio-101512-122326

Cui, Z., Zhao, X., Amevor, F. K., Du, X., Wang, Y., Li, D., Shu, G., Tian, Y., & Zhao, X. (2022). Therapeutic application of quercetin in aging-related diseases: SIRT1 as a potential mechanism. In Frontiers in Immunology (Vol. 13). Frontiers Media S.A. https://doi.org/10.3389/fimmu.2022.943321

de Araújo Boleti, A. P., de Oliveira Flores, T. M., Moreno, S. E., Anjos, L. dos, Mortari, M. R., & Migliolo, L. (2020). Neuroinflammation: An overview of neurodegenerative and metabolic diseases and of biotechnological studies. In Neurochemistry International (Vol. 136). Elsevier Ltd. https://doi.org/10.1016/j.neuint.2020.104714

de Araújo, F. M., Cuenca-Bermejo, L., Fernández-Villalba, E., Costa, S. L., Silva, V. D. A., & Herrero, M. T. (2022). Role of Microgliosis and NLRP3 Inflammasome in Parkinson's Disease Pathogenesis and Therapy. Cellular and Molecular Neurobiology, 42(5), 1283–1300. https://doi.org/10.1007/s10571-020-01027-6

Delenclos, M., Trendafilova, T., Mahesh, D., Baine, A. M., Moussaud, S., Yan, I. K., Patel, T., & McLean, P. J. (2017). Investigation of Endocytic Pathways for the Internalization of Exosome-Associated Oligomeric Alpha-Synuclein. Frontiers in Neuroscience, 11. https://doi.org/10.3389/fnins.2017.00172

Dello Russo, C., Cappoli, N., Coletta, I., Mezzogori, D., Paciello, F., Pozzoli, G., Navarra, P., & Battaglia, A. (2018). The human microglial HMC3 cell line: where do we stand? A systematic literature review. Journal of neuroinflammation, 15(1), 259. https://doi.org/10.1186/s12974-018-1288-0

DiSabato, D. J., Quan, N., & Godbout, J. P. (2016). Neuroinflammation: the devil is in the details. Journal of Neurochemistry, 139, 136–153. https://doi.org/10.1111/jnc.13607

Dixson, A. C., Dawson, T. R., di Vizio, D., & Weaver, A. M. (2023). Context-specific regulation of extracellular vesicle biogenesis and cargo selection. Nature Reviews Molecular Cell Biology, 24(7), 454–476. https://doi.org/10.1038/s41580-023-00576-0

Doyle, L. M., & Wang, M. Z. (2019). Overview of extracellular vesicles, their origin, composition, purpose, and methods for exosome isolation and analysis. In Cells (Vol. 8, Issue 7). MDPI. https://doi.org/10.3390/cells8070727

Eguchi, S., Takefuji, M., Sakaguchi, T., Ishihama, S., Mori, Y., Tsuda, T., Takikawa, T., Yoshida, T., Ohashi, K., Shimizu, Y., Hayashida, R., Kondo, K., Bando, Y. K., Ouchi, N., & Murohara, T. (2019). Cardiomyocytes capture stem cell-derived, anti-apoptotic microRNA-214 via clathrin-mediated endocytosis in acute myocardial infarction. Journal of Biological Chemistry, 294(31), 11665–11674. https://doi.org/10.1074/jbc.RA119.007537

Escrevente, C., Keller, S., Altevogt, P., & Costa, J. (2011). Interaction and uptake of exosomes by ovarian cancer cells. BMC Cancer, 11(1), 108. https://doi.org/10.1186/1471-2407-11-108

Etemad, S., Zamin, R. M., Ruitenberg, M. J., & Filgueira, L. (2012). A novel in vitro human microglia model: characterization of human monocyte-derived microglia. Journal of neuroscience methods, 209(1), 79–89. https://doi.org/10.1016/j.jneumeth.2012.05.025

Fakouri, A., Razavi, Z.-S., Mohammed, A. T., Hussein, A. H. A., Afkhami, H., & Hooshiar, M. H. (2024). Applications of mesenchymal stem cell-exosome components in wound infection healing: new insights. Burns & Trauma, 12. https://doi.org/10.1093/burnst/tkae021

Feng, D., Zhao, W.-L., Ye, Y.-Y., Bai, X.-C., Liu, R.-Q., Chang, L.-F., Zhou, Q., & Sui, S.-F. (2010). Cellular Internalization of Exosomes Occurs Through Phagocytosis. Traffic, 11(5), 675–687. https://doi.org/10.1111/j.1600-0854.2010.01041.x

Fitzner, D., Schnaars, M., van Rossum, D., Krishnamoorthy, G., Dibaj, P., Bakhti, M., Regen, T., Hanisch, U.-K., & Simons, M. (2011). Selective transfer of exosomes from oligodendrocytes to microglia by macropinocytosis. Journal of Cell Science, 124(3), 447–458. https://doi.org/10.1242/jcs.074088

Franzen, C. A., Simms, P. E., van Huis, A. F., Foreman, K. E., Kuo, P. C., & Gupta, G. N. (2014). Characterization of uptake and internalization of exosomes by bladder cancer cells. BioMed Research International, 2014. https://doi.org/10.1155/2014/619829

Fukami, K., Inanobe, S., Kanemaru, K., & Nakamura, Y. (2010). Phospholipase C is a key enzyme regulating intracellular calcium and modulating the phosphoinositide balance. Progress in Lipid Research, 49(4), 429–437. https://doi.org/10.1016/j.plipres.2010.06.001

Ge, Y., Wu, J., Zhang, L., Huang, N., & Luo, Y. (2024). A New Strategy for the Regulation of Neuroinflammation: Exosomes Derived from Mesenchymal Stem Cells. In Cellular and Molecular Neurobiology (Vol. 44, Issue 1). Springer. https://doi.org/10.1007/s10571-024-01460-x

Gómez-Nicola, D., Fransen, N. L., Suzzi, S., & Perry, V. H. (2013). Regulation of Microglial Proliferation during Chronic Neurodegeneration. The Journal of Neuroscience, 33(6), 2481–2493. https://doi.org/10.1523/JNEUROSCI.4440-12.2013

Gonçalves, V. S. S., Rodríguez-Rojo, S., de Paz, E., Mato, C., Martín, T., & Cocero, M. J. (2015). Production of water soluble quercetin formulations by pressurized ethyl acetate-in-water emulsion technique using natural origin surfactants. Food Hydrocolloids, 51, 295–304. https://doi.org/10.1016/j.foodhyd.2015.05.006

Gonda, A., Moyron, R., Kabagwira, J., A. Vallejos, P., & R. Wall, N. (2020). Cellular-Defined Microenvironmental Internalization of Exosomes. In Extracellular Vesicles and Their Importance in Human Health. IntechOpen. https://doi.org/10.5772/intechopen.86020

Gordon, S. (2016). Phagocytosis: An Immunobiologic Process. Immunity, 44(3), 463–475. https://doi.org/10.1016/j.immuni.2016.02.026

Guan, S., Li, Q., Liu, P., Xuan, X., & Du, Y. (2014). Experimental immunology Umbilical cord blood-derived dendritic cells loaded with BGC823 tumor antigens and DC-derived exosomes stimulate efficient cytotoxic T-lymphocyte responses and antitumor immunity in vitro and in vivo. Central European Journal of Immunology, 2, 142–151. https://doi.org/10.5114/ceji.2014.43713

Gunasegaran, B., Krishnamurthy, S., Chow, S. S., Villanueva, M. D., Guller, A., Ahn, S. B., & Heng, B. (2025). Comparative Analysis of HMC3 and C20 Microglial Cell Lines Reveals Differential Myeloid Characteristics and Responses to Immune Stimuli. Immunology, 175(1), 84–102. https://doi.org/10.1111/imm.13900

Gurunathan, S., Kang, M.-H., & Kim, J.-H. (2021). A Comprehensive Review on Factors Influences Biogenesis, Functions, Therapeutic and Clinical Implications of Exosomes. International Journal of Nanomedicine, Volume 16, 1281–1312. https://doi.org/10.2147/IJN.S291956

Gurung, S., Perocheau, D., Touramanidou, L., & Baruteau, J. (2021). The exosome journey: from biogenesis to uptake and intracellular signalling. Cell Communication and Signaling, 19(1), 47. https://doi.org/10.1186/s12964-021-00730-1

Guzman-Martinez, L., Maccioni, R. B., Andrade, V., Navarrete, L. P., Pastor, M. G., & Ramos-Escobar, N. (2019). Neuroinflammation as a common feature of neurodegenerative disorders. In Frontiers in Pharmacology (Vol. 10, Issue SEP). Frontiers Media S.A. https://doi.org/10.3389/fphar.2019.01008

Halbutoğulları, Z. S., Ece, Z., Korun, U., Demir, C. S., Can Kılıç, K., Alper, B., & Yazır, Y. (2023). OPTIMIZATION OF PROTEIN QUANTIFICATION IN WHARTON JELLY-DERIVED MESENCHYMAL STEM CELL EXOSOMES WHARTON JELİ MEZENKİMAL KÖK HÜCRE EKZOZOMLARINDA PROTEİN MİKTARININ OPTİMİZASYONU. 6(6).

https://doi.org/10.53446/actamednicomedia.1364018

Han, X., Xu, T., Fang, Q., Zhang, H., Yue, L., Hu, G., & Sun, L. (2021). Quercetin hinders microglial activation to alleviate neurotoxicity via the interplay between NLRP3 inflammasome and mitophagy. Redox Biology, 44. https://doi.org/10.1016/j.redox.2021.102010

Harrell, C. R., Volarevic, A., Djonov, V., & Volarevic, V. (2021). Mesenchymal stem cell-derived exosomes as new remedy for the treatment of neurocognitive disorders. In International Journal of Molecular Sciences (Vol. 22, Issue 3, pp. 1–13). MDPI AG. https://doi.org/10.3390/ijms22031433

Harry, G. J., & Kraft, A. D. (2012). Microglia in the developing brain: A potential target with lifetime effects. In NeuroToxicology (Vol. 33, Issue 2, pp. 191–206). https://doi.org/10.1016/j.neuro.2012.01.012

He, A., Wang, M., Li, X., Chen, H., Lim, K., Lu, L., & Zhang, C. (2023). Role of Exosomes in the Pathogenesis and Theranostic of Alzheimer's Disease and Parkinson's Disease. In International Journal of Molecular Sciences (Vol. 24, Issue 13). Multidisciplinary Digital Publishing Institute (MDPI). https://doi.org/10.3390/ijms241311054

Heijnen, H. F., Schiel, A. E., Fijnheer, R., Geuze, H. J., & Sixma, J. J. (1999). Activated platelets release two types of membrane vesicles: microvesicles by surface shedding and exosomes derived from exocytosis of multivesicular bodies and alpha-granules. Blood, 94(11), 3791–3799.

Helmut, K., Hanisch, U. K., Noda, M., & Verkhratsky, A. (2011). Physiology of microglia. Physiological Reviews, 91(2), 461–553. https://doi.org/10.1152/physrev.00011.2010

Henne, W. M., Buchkovich, N. J., & Emr, S. D. (2011). The ESCRT Pathway. Developmental Cell, 21(1), 77–91. https://doi.org/10.1016/j.devcel.2011.05.015

Heusermann, W., Hean, J., Trojer, D., Steib, E., von Bueren, S., Graff-Meyer, A., Genoud, C., Martin, K., Pizzato, N., Voshol, J., Morrissey, D. v., Andaloussi, S. E. L., Wood, M. J., & Meisner-Kober, N. C. (2016). Exosomes surf on filopodia to enter cells at endocytic hot spots, traffic within endosomes, and are targeted to the ER. Journal of Cell Biology, 213(2), 173–184. https://doi.org/10.1083/jcb.201506084

Isik, S., Yeman Kiyak, B., Akbayir, R., Seyhali, R., & Arpaci, T. (2023). Microglia Mediated Neuroinflammation in Parkinson's Disease. In Cells (Vol. 12, Issue 7). MDPI. https://doi.org/10.3390/cells12071012

Jembrek, M. J., Oršolić, N., Mandić, L., Sadžak, A., & Šegota, S. (2021). Anti-oxidative, anti-inflammatory and anti-apoptotic effects of flavonols: Targeting nrf2, nf-κb and p53 pathways in neurodegeneration. In Antioxidants (Vol. 10, Issue 10). MDPI. https://doi.org/10.3390/antiox10101628

Joshi, B. S., de Beer, M. A., Giepmans, B. N. G., & Zuhorn, I. S. (2020). Endocytosis of Extracellular Vesicles and Release of Their Cargo from Endosomes. ACS Nano, 14(4), 4444–4455. https://doi.org/10.1021/acsnano.9b10033

Kalluri, R., & LeBleu, V. S. (2020). The biology , function , and biomedical applications of exosomes. Science, 367(6478). https://doi.org/10.1126/science.aau6977

Kang, C. H., Choi, Y. H., Moon, S. K., Kim, W. J., & Kim, G. Y. (2013). Quercetin inhibits lipopolysaccharide-induced nitric oxide production in BV2 microglial cells by suppressing the NF-κB pathway and activating the Nrf2-dependent HO-1 pathway. International Immunopharmacology, 17(3), 808–813. https://doi.org/10.1016/j.intimp.2013.09.009

Kerr, M. C., & Teasdale, R. D. (2009). Defining Macropinocytosis. Traffic, 10(4), 364–371. https://doi.org/10.1111/j.1600-0854.2009.00878.x

Kiss, A. L., & Botos, E. (2009). Endocytosis via caveolae: alternative pathway with distinct cellular compartments to avoid lysosomal degradation? Journal of Cellular and Molecular Medicine, 13(7), 1228–1237. https://doi.org/10.1111/j.1582-4934.2009.00754.x

Klumperman, J., & Raposo, G. (2014). The Complex Ultrastructure of the Endolysosomal System. Cold Spring Harbor Perspectives in Biology, 6(10), a016857–a016857. https://doi.org/10.1101/cshperspect.a016857

Krylova S. V., & Feng, D. (2023). The Machinery of Exosomes: Biogenesis, Release, and Uptake. In International Journal of Molecular Sciences (Vol. 24, Issue 2). MDPI. https://doi.org/10.3390/ijms24021337

Kwon, H. S., & Koh, S. H. (2020). Neuroinflammation in neurodegenerative disorders: the roles of microglia and astrocytes. In Translational Neurodegeneration (Vol. 9, Issue 1). BioMed Central Ltd. https://doi.org/10.1186/s40035-020-00221-2

Lai, R. C., Tan, S. S., Teh, B. J., Sze, S. K., Arslan, F., de Kleijn, D. P., Choo, A., & Lim, S. K. (2012). Proteolytic Potential of the MSC Exosome Proteome: Implications for an Exosome-Mediated Delivery of Therapeutic Proteasome. International Journal of Proteomics, 2012, 1–14. https://doi.org/10.1155/2012/971907

Lamptey, R. N. L., Chaulagain, B., Trivedi, R., Gothwal, A., Layek, B., & Singh, J. (2022). A Review of the Common Neurodegenerative Disorders: Current Therapeutic Approaches and the Potential Role of Nanotherapeutics. In International Journal of Molecular Sciences (Vol. 23, Issue 3). MDPI. https://doi.org/10.3390/ijms23031851

Lee, Y. J., Shin, K. J., & Chae, Y. C. (2024). Regulation of cargo selection in exosome biogenesis and its biomedical applications in cancer. Experimental & Molecular Medicine, 56(4), 877–889. https://doi.org/10.1038/s12276-024-01209-y

Lehmann, M. J., Sherer, N. M., Marks, C. B., Pypaert, M., & Mothes, W. (2005). Actin- and myosin-driven movement of viruses along filopodia precedes their entry into cells. The Journal of Cell Biology, 170(2), 317–325. https://doi.org/10.1083/jcb.200503059

Li, H., Zhang, X., Chen, M., Chen, J., Gao, T., & Yao, S. (2018). Dexmedetomidine inhibits inflammation in microglia cells under stimulation of LPS and ATP by c-Fos/NLRP3/caspase-1 cascades. EXCLI journal, 17, 302–311. https://doi.org/10.17179/excli2017-1018

Lim, J. P., & Gleeson, P. A. (2011). Macropinocytosis: an endocytic pathway for internalising large gulps. Immunology & Cell Biology, 89(8), 836–843. https://doi.org/10.1038/icb.2011.20

Lively, S., & Schlichter, L. C. (2013). The microglial activation state regulates migration and roles of matrix-dissolving enzymes for invasion. Journal of Neuroinflammation, 10(1), 843. https://doi.org/10.1186/1742-2094-10-75

Lötvall, J., Hill, A. F., Hochberg, F., Buzás, E. I., di Vizio, D., Gardiner, C., Gho, Y. S., Kurochkin, I. v., Mathivanan, S., Quesenberry, P., Sahoo, S., Tahara, H., Wauben, M. H., Witwer, K. W., & Théry, C. (2014). Minimal experimental requirements for definition of extracellular vesicles and their functions: a position statement from the International Society for Extracellular Vesicles. Journal of Extracellular Vesicles, 3(1). https://doi.org/10.3402/jev.v3.26913

Martins, T. S., Catita, J., Rosa, I. M., da Cruz e Silva, O. A. B., & Henriques, A. G. (2018). Exosome isolation from distinct biofluids using precipitation and column-based approaches. PLoS ONE, 13(6). https://doi.org/10.1371/journal.pone.0198820

Mattila, P. K., & Lappalainen, P. (2008). Filopodia: molecular architecture and cellular functions. Nature Reviews Molecular Cell Biology, 9(6), 446–454. https://doi.org/10.1038/nrm2406

Mazgaeen, L., & Gurung, P. (2020). Recent advances in lipopolysaccharide recognition systems. In International Journal of Molecular Sciences (Vol. 21, Issue 2). MDPI AG. https://doi.org/10.3390/ijms21020379

Mettlen, M., Chen, P.-H., Srinivasan, S., Danuser, G., & Schmid, S. L. (2018a). Regulation of Clathrin-Mediated Endocytosis. Annual Review of Biochemistry, 87(1), 871–896. https://doi.org/10.1146/annurev-biochem-062917-012644

Mettlen, M., Chen, P.-H., Srinivasan, S., Danuser, G., & Schmid, S. L. (2018b). Regulation of Clathrin-Mediated Endocytosis. Annual Review of Biochemistry, 87(1), 871–896. https://doi.org/10.1146/annurev-biochem-062917-012644

Mulcahy, L. A., Pink, R. C., & Carter, D. R. F. (2014a). Routes and mechanisms of extracellular vesicle uptake. Journal of Extracellular Vesicles, 3(1). https://doi.org/10.3402/jev.v3.24641

Mulcahy, L. A., Pink, R. C., & Carter, D. R. F. (2014b). Routes and mechanisms of extracellular vesicle uptake. Journal of Extracellular Vesicles, 3(1). https://doi.org/10.3402/jev.v3.24641

Munich, S., Sobo-Vujanovic, A., Buchser, W. J., Beer-Stolz, D., & Vujanovic, N. L. (2012). Dendritic cell exosomes directly kill tumor cells and activate natural killer cells via TNF superfamily ligands. OncoImmunology, 1(7), 1074–1083. https://doi.org/10.4161/onci.20897

Nanbo, A., Kawanishi, E., Yoshida, R., & Yoshiyama, H. (2013). Exosomes Derived from Epstein-Barr Virus-Infected Cells Are Internalized via Caveola-Dependent Endocytosis and Promote Phenotypic Modulation in Target Cells. Journal of Virology, 87(18), 10334–10347. https://doi.org/10.1128/JVI.01310-13

Nifli, A. P., Theodoropoulos, P. A., Munier, S., Castagnino, C., Roussakis, E., Katerinopoulos, H. E., Vercauteren, J., & Castanas, E. (2007). Quercetin exhibits a specific fluorescence in cellular milieu: A valuable tool for the study of its intracellular distribution. Journal of Agricultural and Food Chemistry, 55(8), 2873–2878. https://doi.org/10.1021/jf0632637

Nikfarjam, S., Rezaie, J., Zolbanin, N. M., & Jafari, R. (2020). Mesenchymal stem cell derived-exosomes: a modern approach in translational medicine. In Journal of Translational Medicine (Vol. 18, Issue 1). BioMed Central Ltd. https://doi.org/10.1186/s12967-020-02622-3

Niknam, B., Azizsoltani, A., Heidari, N., Tokhanbigli, S., Alavifard, H., Haji Valili, M., Amani, D., Aghdaei, H. A., Hashemi, S. M., & Baghaei, K. (2024). A Simple High Yield Technique for Isolation of Wharton's Jelly-derived Mesenchymal Stem Cell. Avicenna Journal of Medical Biotechnology. https://doi.org/10.18502/ajmb.v16i2.14860

Palanisamy, C. P., Pei, J. J., Alugoju, P., Anthikapalli, N. V. A., Jayaraman, S., Veeraraghavan, V. P., Gopathy, S., Roy, J. R., Janaki, C. S., Thalamati, D., Mironescu, M., Luo, Q., Miao, Y., Chai, Y., & Long, Q. (2023). New strategies of neurodegenerative disease treatment with extracellular vesicles (EVs) derived from mesenchymal stem cells (MSCs). In Theranostics (Vol. 13, Issue 12, pp. 4138–4165). Ivyspring International Publisher. https://doi.org/10.7150/thno.83066

Pawlikowska-Pawlega, B., Ignacy Gruszecki, W., Misiak, L., Paduch, R., Piersiak, T., Zarzyka, B., Pawelec, J., & Gawron, A. (2007). Modification of membranes by quercetin, a naturally occurring flavonoid, via its incorporation in the polar head group. Biochimica et Biophysica Acta - Biomembranes, 1768(9), 2195–2204. https://doi.org/10.1016/j.bbamem.2007.05.027

Pegtel, D. M., & Gould, S. J. (2019). Exosomes. Annual Review of Biochemistry, 88(1), 487–514. https://doi.org/10.1146/annurev-biochem-013118-111902

Peng, H., Li, Y., Ji, W., Zhao, R., Lu, Z., Shen, J., Wu, Y., Wang, J., Hao, Q., Wang, J., Wang, W., Yang, J., & Zhang, X. (2022). Intranasal Administration of Self-Oriented Nanocarriers Based on Therapeutic Exosomes for Synergistic Treatment of Parkinson's Disease. ACS Nano, 16(1), 869–

884. https://doi.org/10.1021/acsnano.1c08473

Rajput, A., Varshney, A., Bajaj, R., & Pokharkar, V. (2022). Exosomes as New Generation Vehicles for Drug Delivery: Biomedical Applications and Future Perspectives. Molecules, 27(21), 7289. https://doi.org/10.3390/molecules27217289

Rastogi, S., Sharma, V., Bharti, P. S., Rani, K., Modi, G. P., Nikolajeff, F., & Kumar, S. (2021). The Evolving Landscape of Exosomes in Neurodegenerative Diseases: Exosomes Characteristics and a Promising Role in Early Diagnosis. International Journal of Molecular Sciences, 22(1), 440. https://doi.org/10.3390/ijms22010440

Rauf, A., Badoni, H., Abu-Izneid, T., Olatunde, A., Rahman, M. M., Painuli, S., Semwal, P., Wilairatana, P., & Mubarak, M. S. (2022). Neuroinflammatory Markers: Key Indicators in the Pathology of Neurodegenerative Diseases. In Molecules (Vol. 27, Issue 10). MDPI. https://doi.org/10.3390/molecules27103194

Rawlinson, C., Jenkins, S., Thei, L., Dallas, M. L., & Chen, R. (2020). Post-Ischaemic Immunological Response in the Brain: Targeting Microglia in Ischaemic Stroke Therapy. Brain Sciences, 10(3), 159. https://doi.org/10.3390/brainsci10030159

Salehi, B., Machin, L., Monzote, L., Sharifi-Rad, J., Ezzat, S. M., Salem, M. A., Merghany, R. M., el Mahdy, N. M., Kılıç, C. S., Sytar, O., Sharifi-Rad, M., Sharopov, F., Martins, N., Martorell, M., & Cho, W. C. (2020). Therapeutic Potential of Quercetin: New Insights and Perspectives for Human Health. ACS Omega, 5(20), 11849–11872. https://doi.org/10.1021/acsomega.0c01818

Salvi, V., Sozio, F., Sozzani, S., & del Prete, A. (2017). Role of Atypical Chemokine Receptors in Microglial Activation and Polarization. Frontiers in Aging Neuroscience, 9. https://doi.org/10.3389/fnagi.2017.00148

Shabab, T., Khanabdali, R., Moghadamtousi, S. Z., Kadir, H. A., & Mohan, G. (2017). Neuroinflammation pathways: a general review. In International Journal of Neuroscience (Vol. 127, Issue 7, pp. 624–633). Taylor and Francis Ltd. https://doi.org/10.1080/00207454.2016.1212854

Sobo-Vujanovic, A., Munich, S., & Vujanovic, N. L. (2014). Dendritic-cell exosomes cross-present Toll-like receptor-ligands and activate bystander dendritic cells. Cellular Immunology, 289(1–2), 119–127. https://doi.org/10.1016/j.cellimm.2014.03.016

Streit, W. J., Mrak, R. E., & Griffin, W. S. T. (2004). Microglia and neuroinflammation: A pathological perspective. Journal of Neuroinflammation, 1. https://doi.org/10.1186/1742-2094-1-14

Streit, W. J., Walter, S. A., & Pennell, N. A. (1999). Reactive microgliosis. Progress in neurobiology, 57(6), 563–581. https://doi.org/10.1016/s0301-0082(98)00069-0

Stuffers, S., Sem Wegner, C., Stenmark, H., & Brech, A. (2009). Multivesicular Endosome Biogenesis in the Absence of ESCRTs. Traffic, 10(7), 925–937. https://doi.org/10.1111/j.1600-0854.2009.00920.x

Svensson, K. J., Christianson, H. C., Wittrup, A., Bourseau-Guilmain, E., Lindqvist, E., Svensson, L. M., Mörgelin, M., & Belting, M. (2013). Exosome Uptake Depends on ERK1/2-Heat Shock Protein 27 Signaling and Lipid Raft-mediated Endocytosis Negatively Regulated by Caveolin-1. Journal of Biological Chemistry, 288(24), 17713–17724. https://doi.org/10.1074/jbc.M112.445403

Théry, C., Amigorena, S., Raposo, G., & Clayton, A. (2006). Isolation and Characterization of Exosomes from Cell Culture Supernatants and Biological Fluids. Current Protocols in Cell Biology, 30(1). https://doi.org/10.1002/0471143030.cb0322s30

Thomi, G., Surbek, D., Haesler, V., Joerger-Messerli, M., & Schoeberlein, A. (2019). Exosomes derived from umbilical cord mesenchymal stem cells reduce microglia-mediated neuroinflammation in

perinatal brain injury. Stem Cell Research and Therapy, 10(1). https://doi.org/10.1186/s13287-019-1207-z

Tian, Y., Li, S., Song, J., Ji, T., Zhu, M., Anderson, G. J., Wei, J., & Nie, G. (2014). A doxorubicin delivery platform using engineered natural membrane vesicle exosomes for targeted tumor therapy. Biomaterials, 35(7), 2383–2390. https://doi.org/10.1016/j.biomaterials.2013.11.083

Tkach, M., Kowal, J., Zucchetti, A. E., Enserink, L., Jouve, M., Lankar, D., Saitakis, M., Martin-Jaular, L., & Théry, C. (2017). Qualitative differences in T-cell activation by dendritic cell-derived extracellular vesicle subtypes. The EMBO Journal, 36(20), 3012–3028. https://doi.org/10.15252/embj.201696003

Valapala, M., & Vishwanatha, J. K. (2011). Lipid Raft Endocytosis and Exosomal Transport Facilitate Extracellular Trafficking of Annexin A2. Journal of Biological Chemistry, 286(35), 30911–30925. https://doi.org/10.1074/jbc.M111.271155

Verweij, F. J., Bebelman, M. P., Jimenez, C. R., Garcia-Vallejo, J. J., Janssen, H., Neefjes, J., Knol, J. C., de Goeij-de Haas, R., Piersma, S. R., Baglio, S. R., Verhage, M., Middeldorp, J. M., Zomer, A., van Rheenen, J., Coppolino, M. G., Hurbain, I., Raposo, G., Smit, M. J., Toonen, R. F. G., … Pegtel, D. M. (2018). Quantifying exosome secretion from single cells reveals a modulatory role for GPCR signaling. Journal of Cell Biology, 217(3), 1129–1142. https://doi.org/10.1083/jcb.201703206

Vestad, B., Llorente, A., Neurauter, A., Phuyal, S., Kierulf, B., Kierulf, P., Skotland, T., Sandvig, K., Haug, K. B. F., & Øvstebø, R. (2017). Size and concentration analyses of extracellular vesicles by nanoparticle tracking analysis: a variation study. Journal of Extracellular Vesicles, 6(1). https://doi.org/10.1080/20013078.2017.1344087

Weiss, D. J., Bates, J. H. T., Gilbert, T., Liles, W. C., Lutzko, C., Rajagopal, J., & Prockop, D. (2013). Stem cells and cell therapies in lung biology and diseases: Conference report. Annals of the American Thoracic Society, 10(5). https://doi.org/10.1513/AnnalsATS.201304-089AW

Weissman I. L. (2000). Stem cells: units of development, units of regeneration, and units in evolution. Cell, 100(1), 157–168. https://doi.org/10.1016/s0092-8674(00)81692-x

Xiao, L., Hareendran, S., & Loh, Y. P. (2021). Function of exosomes in neurological disorders and brain tumors. Extracellular Vesicles and Circulating Nucleic Acids. https://doi.org/10.20517/evcna.2021.04

Yoon, J. H., Ashktorab, H., Smoot, D. T., Nam, S. W., Hur, H., & Park, W. S. (2020). Uptake and tumor-suppressive pathways of exosome-associated GKN1 protein in gastric epithelial cells. Gastric Cancer, 23(5), 848–862. https://doi.org/10.1007/s10120-020-01068-2

Yu, B., Zhang, X., & Li, X. (2014). Exosomes Derived from Mesenchymal Stem Cells. International Journal of Molecular Sciences, 15(3), 4142–4157. https://doi.org/10.3390/ijms15034142

Zakrzewski, W., Dobrzyński, M., Szymonowicz, M., & Rybak, Z. (2019). Stem cells: Past, present, and future. In Stem Cell Research and Therapy (Vol. 10, Issue 1). BioMed Central Ltd. https://doi.org/10.1186/s13287-019-1165-5

Zhang, W., Xiao, D., Mao, Q., & Xia, H. (2023). Role of neuroinflammation in neurodegeneration development. In Signal Transduction and Targeted Therapy (Vol. 8, Issue 1). Springer Nature. https://doi.org/10.1038/s41392-023-01486-5